Published OnlineFirst October 9, 2013; DOI: 10.1158/1535-7163.MCT-13-0243

Molecular Cancer Therapeutics

BRAF V600E Is a Determinant of Sensitivity to Proteasome Inhibitors

Davide Zecchin, Valentina Boscaro, Enzo Medico, et al.

Mol Cancer Ther 2013;12:2950-2961. Published OnlineFirst October 9, 2013.

Published OnlineFirst October 9, 2013; DOI: 10.1158/1535-7163.MCT-13-0243

Molecular Cancer Therapeutics

BRAF V600E Is a Determinant of Sensitivity to Proteasome Inhibitors

Davide Zecchin[1,3], Valentina Boscaro[2], Enzo Medico[1,3], Ludovic Barault[3], Miriam Martini[1,3], Sabrina Arena[3], Carlotta Cancelliere[3,4], Alice Bartolini[3], Emily H. Crowley[3], Alberto Bardelli[1,3,4], Margherita Gallicchio[2], and Federica Di Nicolantonio[1,3]

Abstract

A critical step toward defining tailored therapy in patients with cancer is the identification of genetic interactions that may impair—or boost—the efficacy of selected therapeutic approaches. Cell models able to recapitulate combinations of genetic aberrations are important to find drug–genotype interactions poorly affected by the heterogeneous genetics of human tumors. In order to identify novel pharmacogenomic relationships, we employed an isogenic cell panel that reconstructs cancer genetic scenarios. We screened a library of 43 compounds in human hTERT-HME1 epithelial cells in which *PTEN* or *RB1* were silenced in combination with the targeted knockin of cancer-associated mutations in *EGFR, KRAS, BRAF*, or *PIK3CA* oncogenes. Statistical analysis and clustering algorithms were applied to display similar drug response profiles and mutation-specific patterns of activity. From the screen, we discovered that proteasome inhibitors show selectivity toward *BRAF* V600E–mutant cells, irrespective of PTEN or RB1 expression. Preferential targeting of *BRAF*-mutant cells by proteasome inhibitors was corroborated in a second *BRAF V600E* isogenic model, as well as in a panel of colorectal cancer cell lines by the use of the proteasome inhibitor carfilzomib. Notably, carfilzomib also showed striking *in vivo* activity in a *BRAF*-mutant human colorectal cancer xenograft model. Vulnerability to proteasome inhibitors is dependent on persistent BRAF signaling, because BRAF V600E blockade by PLX4720 reversed sensitivity to carfilzomib in *BRAF*-mutant colorectal cancer cells. Our findings indicated that proteasome inhibition might represent a valuable targeting strategy in *BRAF* V600E–mutant colorectal tumors. *Mol Cancer Ther; 12(12); 2950–61. ©2013 AACR.*

Introduction

Over the past decade, research has demonstrated that the clinical benefit from targeted therapies is dependent upon our knowledge of the presence of specific genetic aberrations within the tumor (1–9). To maximize therapy efficacy, treatment must be tailored to the genetic milieu of a specific tumor, to deliver what is referred to as 'precision medicine'.

This approach has led to progress in the treatment of specific malignancies including breast cancers overexpressing or harboring amplified EGF receptor 2 (HER-2) that can be successfully treated with trastuzumab (5). In addition, lung cancers carrying specific mutations in the EGF receptor (EGFR) are particularly sensitive to the EGFR tyrosine kinase inhibitors gefitinib and erlotinib (1–4). In addition, recent examples include selective clinical activity of the BRAF inhibitors vemurafenib or dabrafenib in melanomas with *BRAF* V600E mutation (6, 7), or the efficacy of the *ALK* inhibitor crizotinib for the treatment of lung cancers carrying translocation of the anaplastic leukemia kinase (ALK; refs. 8, 9).

However, only approximately 50% of patients with BRAF-mutant melanoma, 30% of patients with HER2-amplified breast cancer, and 60% of patients with EGFR-mutant or ALK-translocated lung cancer respond to blockade of the corresponding targets (1–9). Simple binary relationships between genetic aberrations and drug response are complicated in these cases by the intricate genetic landscape of solid tumors (10). Indeed, in most instances, multiple tumor suppressor mutations and oncogene variants occur in the same solid tumor [http://cancergenome.nih.gov/], and it is thought that,

Authors' Affiliations: Departments of [1]Oncology and [2]Scienza e Tecnologia del Farmaco, University of Torino, Torino; [3]IRCC Institute for Cancer Research and Treatment at Candiolo, Candiolo; and [4]FIRC Institute of Molecular Oncology (IFOM), Milano, Italy

Note: Supplementary data for this article are available at Molecular Cancer Therapeutics Online (http://mct.aacrjournals.org/).

D. Zecchin and V. Boscaro contributed equally to this work.

Current address for D. Zecchin: Signal Transduction Laboratory, Cancer Research UK London Research Institute, London, United Kingdom; and current address for M. Martini, Dipartimento di Biotecnologie Molecolari e Scienze per la Salute, Molecular Biotechnology Center, Torino, Italy.

Corresponding Authors: Federica Di Nicolantonio, Department of Oncology, University of Torino, Institute for Cancer Research and Treatment at Candiolo, Strada Provinciale 142 Km 3.95, Candiolo, I-10060, Turin, Italy. Phone: 39-011-9933827; Fax 39-011-9933225; E-mail: federica.dinicolantonio@unito.it; and Margherita Gallicchio, margherita.gallicchio@unito.it

doi: 10.1158/1535-7163.MCT-13-0243

Published OnlineFirst October 9, 2013; DOI: 10.1158/1535-7163.MCT-13-0243

together, these molecular alterations contribute to patients' response to specific anticancer treatment. It has been reported, for instance, that the sensitivity of the *EGFR*-mutant lung cancer cells to EGFR tyrosine kinase inhibitors is reduced by inactivation of PTEN (11, 12). The activation of the phosphoinositide 3-kinase (PI3K) pathway, defined by PTEN loss and/or *PIK3CA* mutation, was also associated with poor response to trastuzumab and shorter survival time in HER-2–positive metastatic breast cancer (13, 14). This indicates that the influence of tumor complex genetics on therapy response warrants further consideration.

Nevertheless, there is a paucity of functional studies that systematically evaluate the effect of complex genotypes in the modulation of drug responses. We believe that such experimental approaches are fundamental in order to identify novel drug-genotype interactions that are unaffected by the concomitant presence of other common genetic alterations. On the other hand, these studies may improve our ability to predict response to existing anticancer therapies based on the plethora of genetic aberrations present in a solid tumor.

In this report, we employed a previously characterized panel of isogenic human cell lines that recreate possible molecular scenarios observed in human cancer (15). Using a homologous recombination, we introduced the activating mutations *EGFR* delE746-A750, *PIK3CA* H1047R, *PIK3CA* E545K, *KRAS* G13D, and *BRAF* V600E into the genome of the nontransformed human cell line hTERT-HME-1 (abbreviated as HME-1), which already harbors the C176F on *TP53*. This *TP53* mutation was previously reported to impair the TP53 checkpoint response to genotoxic stress in HME-1 cells (15). *PTEN* or *RB1* tumor suppressor genes have been systematically silenced in these isogenic cell lines generating a combinatorial model referred to as the "matrix" (See Supplementary Fig. S1).

Using the HME-1 matrix, we investigated the role of single or multiple cancer genetic alterations in modulating the response to antineoplastic drugs. This approach uncovered a novel pharmacogenetic interaction between proteasome inhibitors and the *BRAF* V600E allele.

The *BRAF* V600E mutation occurs in 5% to 8% of advanced colorectal cancer samples. Patients with metastatic colorectal cancer with *BRAF*-mutant tumors have a poor prognosis and do not respond to BRAF inhibitors in monotherapy (16, 17). Accordingly, the development of therapeutic strategies for metastatic *BRAF* mutated colorectal cancer represent an urgent and unmet clinical need. We, therefore, elected to evaluate the activity of proteasome inhibitors in *BRAF*-mutant colorectal cancer models. Finally, we investigated the ability of selective BRAF targeted agents to modulate response to the proteasome inhibitor carfilzomib in *BRAF*-mutant colorectal cancer cells.

Materials and Methods

Cells and cell culture reagents

The HME-1 cell line was obtained from the American Type Culture Collection (ATCC; LGC Standards S.r.l, Milan, Italy) in October 2005. The CACO2, NCI-H716, HuTu80, COLO201, SW1417, and LS411N cell lines were purchased from the ATCC in June 2010; COLO320 and HCA7 were obtained from the European Collection of Cell Cultures (ECACC) in September 2009 (distributed by Sigma-Aldrich Srl, Milan, Italy). CaR1 and OUMS23 cell lines were purchased from the Japanese Collection of Research Bioresources (JCRB) (Tokyo, Japan) in January 2011. The HDC135 cell line was obtained from the German Collection of Microorganisms and Cell Cultures (DSMZ) repository (Braunschweig, Germany) in November 2010. The NCI-H630, KM20, and SNU-C5 cell lines were purchased from the Korean Cell Bank (Seoul, Korea) in February 2011. VACO432 and RKO cells were obtained from Horizon Discovery (Cambridge, United Kingdom) in March 2011. The LIM1215, LIM2405, and LIM2537 cell lines (18, 19) were provided by Prof. R. Whitehead, Vanderbilt University, Nashville, with permission from the Ludwig Institute for Cancer Research, Melbourne branch, Australia in August 2011. The DiFi and OXCO1 cell lines were a kind gift from Dr J. Baselga in November 2004 (Oncology Department of Vall d'Hebron University Hospital, Barcelona, Spain) and Dr V. Cerundolo in March 2010 (Weatherall Institute of Molecular Medicine, University of Oxford, Oxford, United Kingdom), respectively. The genetic identity of the cell lines used in this study was confirmed by STR profiling (Cell ID, Promega) no longer than 6 months before drug-profiling experiments. All cells were cultured as previously described (15) or according to the manufacturers' instructions. All cell culture media were supplemented with 10% FBS or 5% for HME-1 (Sigma-Aldrich), 50 U/mL penicillin, and 50 mg/mL streptomycin. Geneticin (G418) was purchased from Gibco and puromycin from Sigma-Aldrich.

Construction of isogenic models

The generation of the HME-1 matrix has been previously reported (15). All experimental procedures for *BRAF* V600E targeting vector construction, adeno-associated virus (AAV) production, cell infection, and screening for recombinants have been described previously (20, 21).

Drug proliferation assay

Parental and mutated cells were seeded in 100 μL complete growth medium at a density of 3×10^3 cells/well in 96-well plastic culture plates. After serial dilutions, 100 μL of drugs in serum-free medium were added to cells with a multichannel pipette. Vehicle- and medium-only–containing wells were added as controls. Plates were incubated at 37°C in 5% CO_2 for 96 hours, after which cell viability was assessed by ATP content using the CellTiter-Glo Luminescent Assay (Promega). To account for clonal variability, two independent isogenic knockin (KI) clones infected with scramble short hairpin RNA (shRNA), or with shRNAs targeting *PTEN* or *RB1* were tested. All luminescence measurements [indicated as relative light units (RLU)] were recorded by the Victor X4 Multilabel Plate Reader (PerkinElmer). In Supplementary

Published OnlineFirst October 9, 2013; DOI: 10.1158/1535-7163.MCT-13-0243

Table S1, we have reported a list of tested compounds, their chemical formula, their molecular weight (MW), the solvent used for suspension, the concentration of stock solutions, the concentrations tested in the experiments, and the storage conditions used for the stock. Each compound was preliminarily tested on HME-1 parental cells infected with scramble shRNA to determine the concentration referred to as the highest no-observed effect level (NOEL), the IC_{50}, and the IC_{90} values, as previously reported (20). The three concentrations of each compound tested on the entire isogenic cell panel were selected on the basis of these premises.

Proteasome activity assay

Proteasome activity was assayed using Proteasome-Glo Chymotrypsin-Like Cell-Based Assay (Promega). Cells were seeded 16 hours prior to drug treatment. Proteasome activity was measured after 2-hour incubation with proteasome inhibitors, according to the manufacturer's instructions.

SDS-PAGE and Western blot analysis

Cell lysates were prepared in boiled Laemmli buffer (2.5% SDS, 125 mmol/L Tris–HCl, pH 6.8). Lysates were sonicated, cleared by centrifugation at 14,000 rpm for 10 minutes at room temperature, and the supernatant containing soluble protein was removed. The protein concentration of the supernatant was determined by micro-BCA protein assay (Pierce). An equal amount (25 μg) of whole-cell lysate per lane was boiled in lithium dodecyl sulfate (LDS) buffer and reducing agent, according to the manufacturers' instructions, and separated by SDS-PAGE on 10% precasted polyacrylamide mini-gels (Invitrogen). The separated lysates were then transferred to a nitrocellulose membrane. The blot was incubated with blocking buffer [Tris-buffered saline (TBS)–10% BSA] for 1 hour at room temperature and incubated overnight with the primary antibody (diluted according to the manufacturer's instructions in TBS–5% BSA) at 4°C. The blot was then washed 3 times for 10 minutes in washing buffer (TBS containing 0.2% Tween 20), incubated with secondary antibody horseradish peroxidase (HRP)-conjugate (Sigma; diluted 1:10,000–1:2,000) and washed a further 3 times. ECL solution (Enhanced Chemioluminescence System, Amersham) was then added to the filter, and the chemiluminescent signal was acquired by the LAS4000 Image reader (Fujifilm). Antibodies used for immunoblotting were: anti-P21, anti-PARP, anti-PTEN, and anti-RB1 (Cell Signaling Technology); anti-EGFR (clone 13G8, Enzo Life Sciences); anti-Ubiquitin (Santa Cruz Biotechnology); and anti–actin (Sigma-Aldrich).

Pharmacology data analysis ("Pharmarray")

Cell viability at each drug concentration was initially normalized to vehicle-treated cells for each cell line, and triplicate observations within the same experiment were averaged. We then calculated, within each experiment, the drug response as follows: we considered the difference between the Log2 viability of the parental cell line and the Log2 viability of a given mutant/genotype. All drug concentrations were tested on each cell line at least 3 times. Drug responses associated to a given mutant and obtained in individual experiments were considered as distinct entities in the subsequent clustering analysis. Similarly, responses to different concentrations of each compound were analyzed as distinct elements in the clustering experiments. All data were clustered and visualized using the publicly available GEDAS software (ref. 22; http://sourceforge.net/projects/gedas).

An array of data was generated in which the red color indicates higher sensitivity (i.e., lower Log2 viability respect to the parental cell line) of a given mutant to a specific drug concentration whereas the green color indicates lower sensitivity (i.e., higher Log2 viability respect to the parental cell line).

The genotypes of the cell lines tested in individual experiments were displayed on the horizontal axis, and we performed an unsupervised, average linkage hierarchic clustering by an uncentered Pearson correlation coefficient. Different drug concentrations were listed in the vertical axis and clustered by the C-means Fuzzy algorithm using an average cosine correlation coefficient. The different clustering metrics were chosen based on the results of the clustering optimization tool included in GEDAS.

Combination effects of PLX4720 and carfilzomib were assessed using the method established by Poch and colleagues (23). We elected to employ the methods of Poch and colleagues as they propose a corrective factor for dose–response curves having a slope different from 1, such as those shown by PLX4720 in most *BRAF*-mutant colorectal cancer cell lines. For this reason, the Poch method results in a more accurate estimation of combination effects when the agents show a relatively flat dose–response curve.

Statistical analysis

Unsupervised clustering analysis was paralleled by statistical evaluation of the genotype-specific differences of the drug responses performed by a *t* test. Specifically, the statistical test compared the responses of the different mutant cell lines to a given compound with the response of the wild-type (WT) scramble control cells. With this aim, a heteroscedastic two-tailed *t* test was employed for all mutants as well as for all compounds (see Supplementary Table S2 for the complete list of *t* tests). In the other experiments, statistically significant differences between groups were determined by using the heteroscedastic Student two-tailed *t* test. A *P* value less than 0.05 was considered statistically significant.

Xenograft studies

All animal procedures were approved by the Ethical Commission of the Institute for Cancer Research and Treatment and by the Italian Ministry of Health. RKO cells were injected subcutaneously into the right posterior

Published OnlineFirst October 9, 2013; DOI: 10.1158/1535-7163.MCT-13-0243

flanks of 7-week-old female CD-1 nude mice (six animals per group; Charles River, Calco, Italy). Tumor volumes were determined using $[D \times (d_2)]/2$, in which D represents the largest diameter of the tumor, and d represents the largest perpendicular volume to D. When tumors reached a volume of approximately 200 to 250 mm^3, mice were randomly assigned to treatment with vehicle or drug. For *in vivo* experiments, carfilzomib was formulated in an aqueous solution of 10% (w/v) sulfobutylether-b-cyclodextrin (Captisol, a free gift from CYDEX Pharmaceuticals Inc) and 10 mmol/L sodium citrate (pH 3.5). Carfilzomib solutions were diluted daily with vehicle before tail-vein injections. Carfilzomib was administered on days 1, 2, 8, 9, 15, and 16 in 28-day cycles at a dose of 4 mg/kg.

Results

The isogenic "matrix" of genotypes recapitulates known interactions between drugs and multiple genetic alterations

We initially assessed whether the HME-1 cellular matrix could recapitulate pharmacogenomic relationships previously established experimentally and clinically.

Previous research showed that EGFR kinase inhibitors are more effective in cells carrying *EGFR* mutations, but the concomitant loss of PTEN impairs this response (11, 12).

Therefore, we focused on HME-1 isogenic cell lines KI for the *EGFR* E746-A750 allele and on their isogenic counterpart lacking PTEN expression. We evaluated the genotype-dependent response of these models to EGFR tyrosine kinase inhibitors as a test case.

We observed that erlotinib, canertinib, and lapatinib, classified as inhibitors of the HER family receptor tyrosine kinase, as well as the dual EGFR–VEGFR inhibitor vandetanib affected the growth of HME-1 isogenic cell lines in which the *EGFR* E746-A750 allele was knocked in. Concomitant inactivation of PTEN partially rescued this phenotype (Fig. 1A and B).

In addition, we observed that the KI of *BRAF* V600E allele conferred resistance to EGFR inhibitors (Fig. 1A) confirming previous findings (24, 25).

These results indicate that HME-1 isogenic models harboring multiple genetic alterations can recapitulate complex drug–genotype relationships found in patients.

Drug screening of isogenic cell lines carrying combinations of genetic alterations

Next, we exploited the isogenic HME-1 matrix to seek novel pharmacogenetic interactions.

We assembled a library of 43 compounds (Supplementary Table S3), including: (i) molecules targeting tyrosine kinase receptors (RTK) or their effectors (e.g., anti-HERs, anti-MEK, anti-SRC, anti-AKT, anti-mTOR); (ii) compounds that do not target members of the RTK signaling pathways, but are employed as anticancer therapies (PARP, proteasome, HSP90 inhibitors, epigenetic modulators); (iii) drugs in clinical use aside from cancer therapy but that have been shown to have antiproliferative and antineoplastic activity (indomethacin, statins). Most of the drugs included in the list are approved by the U.S. Food and Drug Administration (FDA)/European Medicines Agency (EMA) or are undergoing clinical trials in patients with cancer.

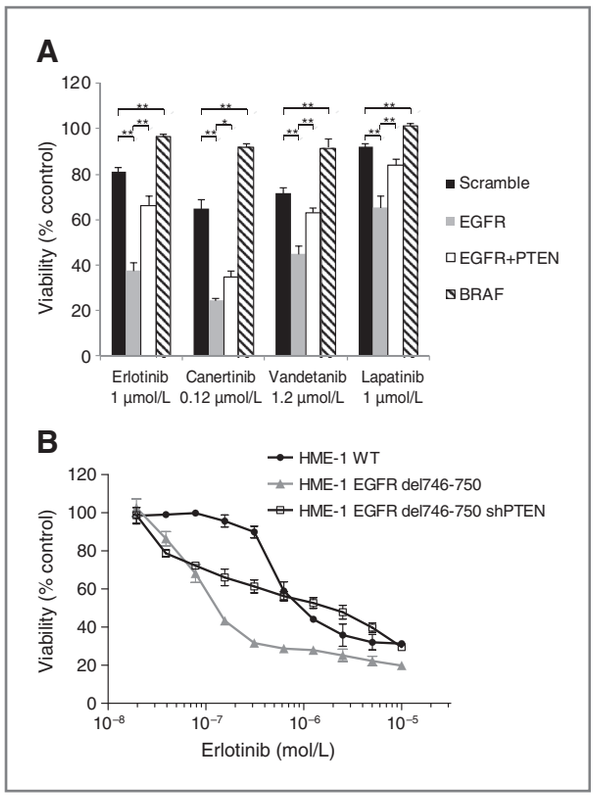

Figure 1. HME-1–mutant cells display drug responses resembling those of tumors carrying equivalent mutations. A, the effect of erlotinib, canertinib, vandetanib, or lapatinib treatment on cellular proliferation was assessed for HME-1 isogenic clones carrying the indicated mutations. Drugs were used at the given concentrations. Cell viability was estimated by determining ATP content in three replicate wells. Results are normalized to the growth of cells treated with dimethyl sulfoxide (DMSO) and are represented as mean ± SEM of at least three independent experiments. B, multiple concentrations of erlotinib were tested on HME-1 isogenic clones carrying the indicated mutations. Cell viability was evaluated by determining ATP content in three replicate wells. Results are normalized to the growth of cells treated with DMSO, and are represented as mean ± SD of one representative experiment out of three. *P* values were determined by Student *t* test. *, $P < 0.01$; **, $P < 0.001$.

Each compound was tested on parental HME-1 cells and on their derivatives infected with a scramble (nontarget) shRNA to verify whether and to what extent infection by lentivirus impacted drug response. No significant differences in response were detected (data not shown). Furthermore, no significant differences were also observed when we evaluated the effect of lentiviral infection on proliferation of the KI cells carrying oncogenic mutations in *KRAS*, *BRAF*, *PIK3CA*, or *EGFR* as compared with their WT counterpart (Supplementary Fig. S2).

Published OnlineFirst October 9, 2013; DOI: 10.1158/1535-7163.MCT-13-0243

The matrix was subsequently assayed for drug responses by a proliferation assay, using at least three drug concentrations and two clones for each different KI genotype. All drugs were tested at least 3 times on each cell line. Drug responses of mutant cells were normalized to the response of parental scramble HME-1 as described in the Materials and Methods section. Normalized data was then clustered and plotted on an array using the GEDAS software (22). This approach was previously developed and described for the analysis of differential drug activity in KI isogenic models and is defined as a "Pharmarray" (20). Cell lines and drugs were clustered on the basis of their response profile. The entire analyzed dataset is shown in Supplementary Fig. S3. Magnification of a drug cluster is shown in Fig. 2 as a relevant example. The Pharmarray analysis revealed that, in most cases, the genotypes sharing a KI mutation or a knocked down tumor suppressor gene were clustered together.

The presence of these clusters suggested that the genotype of HME-1 isogenic models strongly influenced the pattern of response of these cells to the compounds.

BRAF-mutant isogenic HME-1 cells show increased sensitivity to proteasome inhibitors

The cluster of drugs in Fig. 2 preferentially inhibited the *PIK3CA* E545K, *KRAS* G13D, and *BRAF* V600E mutated genotypes. Intriguingly, this cluster of compounds included three different concentrations of the proteasome inhibitor bortezomib. We focused further on the effect of this compound toward *BRAF*-mutant cells, as this drug–genotype interaction was the most novel in our panel and of potential translational relevance. Indeed, no influence of PTEN or RB1 knockdown on bortezomib activity was observed in the cluster.

The preferential targeting of HME-1 *BRAF* KI clones by proteasome inhibitors was confirmed using the nonboronic agent carfilzomib (Fig. 3A and B). These results pointed at proteasome *per se* as a key molecular determinant of the pharmacologic response.

In order to elucidate the relationship between *BRAF* mutated cell lines and proteasome inhibitors, we measured the amount of ubiquitinated proteins following bortezomib treatment. We found that *BRAF*-mutant cells accumulated more ubiquitinated protein with respect to the WT counterpart (Fig. 3C). This was also observed following carfilzomib treatment (Supplementary Fig. S4).

Treatment of HME-1 *BRAF* V600E with clinically relevant concentrations of bortezomib resulted in increased p21 levels and PARP cleavage (Fig. 3C). Proteasome inhibitors appear, therefore, to elicit a greater growth inhibitory and apoptotic response in *BRAF* V600E KI cell lines likely due to an accumulation in ubiquitinated protein.

Increased accumulation of ubiquitinated protein in *BRAF* KI cell lines following treatment with proteasome inhibitors may be due to a higher basal proteasome activity in these cells. To investigate this hypothesis, we measured the proteasome activity in WT versus *BRAF* V600E cell lines under basal conditions and following proteasome inhibitor treatment. To this aim, we employed a cell-based proteasome activity assay, which determines the chymotrypsin-like activity associated with intact proteasomes toward a luminogenic peptide substrate. We showed that *BRAF* mutated HME-1 had higher basal chymotrypsin-like activity with respect to WT cells under basal conditions. Bortezomib treatment reduced activity to comparable levels in all isogenic cell lines (Fig. 3D). The greater fold inhibition of proteasome activity correlates with the increased rate of ubiquitinylated protein accumulation in *BRAF* V600E with respect to the WT.

BRAF-mutant colorectal cancer cells display increased sensitivity to proteasome inhibitors

We then elected to assess the interaction between BRAF inhibitors and response to proteasome inhibitors in colorectal cancer, a malignancy in which the *BRAF* mutation confers poor prognosis in the metastatic setting. To this end, we generated a *BRAF* V600E isogenic cell line using LIM1215 cells, which are WT for *KRAS*, *BRAF*, and *PIK3CA* (18, 26). Using a previously developed methodology (20), we infected LIM1215 cells with a recombinant adeno-associated viral vector carrying the *BRAF* V600E allele. After selection, we isolated two independent clones in which the mutation was introduced (KI) by homologous recombination in heterozygosity under the gene's own promoter. Bortezomib and carfilzomib preferentially inhibited the growth of *BRAF* KI clones with respect to the parental counterpart (Fig. 4A and B). This confirmed that our findings in the breast cancer HME-1 matrix can also be applied to the colorectal cancer cell line LIM1215.

Taking advantage of recent molecular profiling efforts in which the genomic landscape of a large panel of cell lines were characterized (27, 28), we sought to further validate this pharmacogenomic relationship using 12 colorectal cancer cell lines harboring *BRAF* V600E mutations. In addition, we selected eight colorectal cancer cell lines WT for *BRAF* and *KRAS* as negative controls. We independently verified by Sanger sequencing the mutational status of selected hotspots, including *BRAF* exon 15, *KRAS* exons 2-3-4, *NRAS* exons 2–3, and *PIK3CA* exons 9–20. We observed that colorectal cancer cell lines with *BRAF* V600E mutations were particularly responsive to carfilzomib, whereas WT cells were significantly less affected ($P < 0.05$; Fig. 4C). In addition, we showed that sensitivity to carfilzomib is independent of the PTEN or RB1 expression status in colorectal cancer cell lines (Fig. 4D).

These results confirmed that oncogenic *BRAF* is a novel determinant of sensitivity to proteasome inhibitors. However, the presence of few outlier nonresponder cell lines highlighted the potential influence of additional factors, beyond PTEN or RB1 in shaping drug response.

We have recently proposed that EGFR expression can be a determinant of resistance to BRAF or MEK inhibitors in *BRAF*-mutant colorectal cancer cells (29). We asked whether EGFR expression could also be related to the lack of activity of the proteasome inhibitor in some colorectal cancer models. However, we did not detect any

Published OnlineFirst October 9, 2013; DOI: 10.1158/1535-7163.MCT-13-0243

association between response to carfilzomib and EGFR expression in this panel of cancer cells, independently from *BRAF* status (Fig. 4D).

Next, we sought to investigate whether the addiction of *BRAF*-mutant cells to proteasome function was dependent upon the activity of the BRAF V600E–mutant

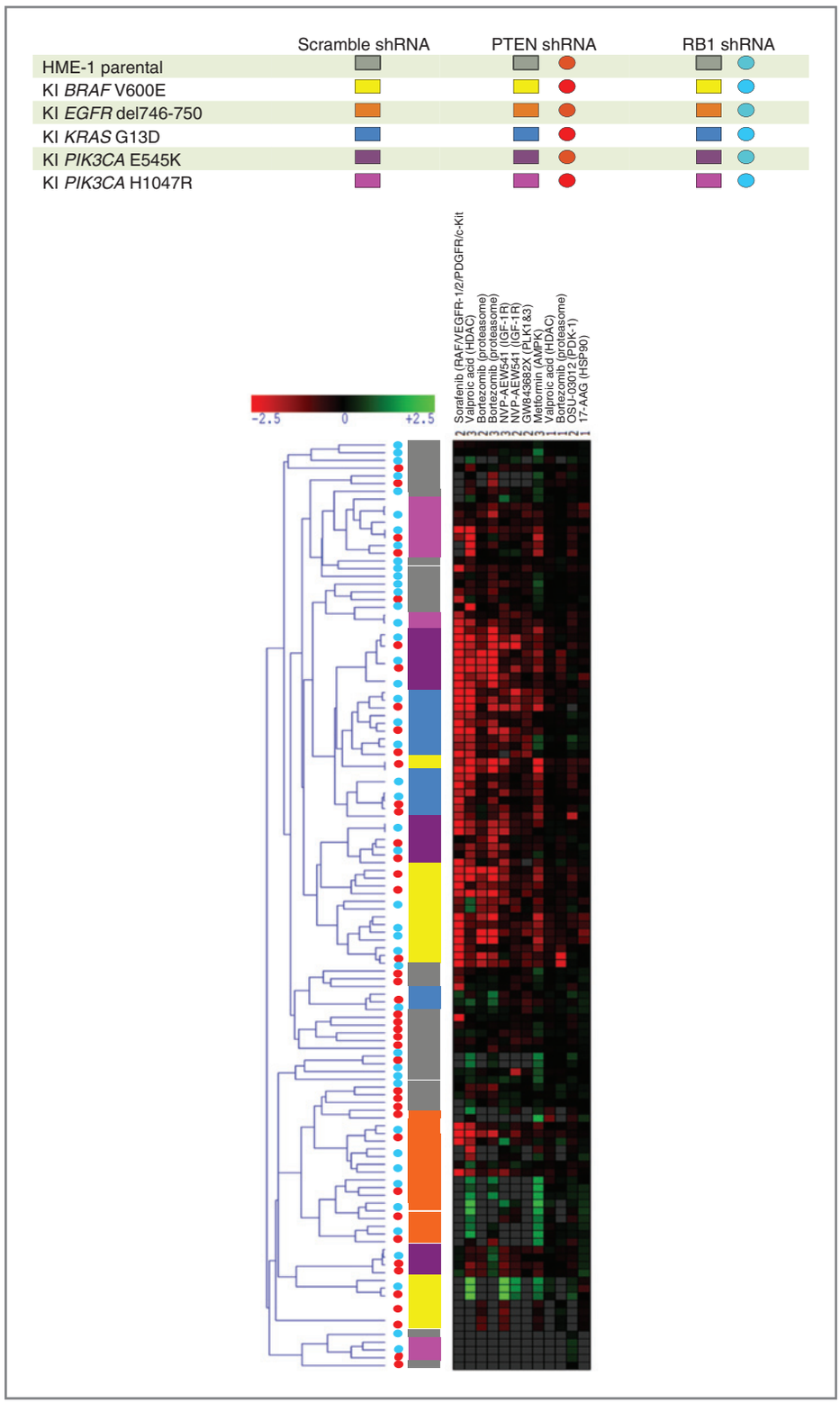

Figure 2. Drug profiling of isogenic HME-1 cells uncovers bortezomib as a preferential inhibitor of *BRAF*/*KRAS*/*PIK3CA*–mutant cells. Magnification of a drug cluster from the Pharmarray panel. The cell line genotype is shown on the vertical axis. Genotypes are defined according to the color code indicated in the legend. Cells carrying the indicated genetic alterations were clustered using a hierarchic unsupervised algorithm based on their response profile versus the whole library; drug names included in the cluster are listed on the horizontal axis at the top of the panel. For each compound, the lowest concentration used was annotated with the number 1, intermediate concentration with 2, and the highest with 3. The drug name is followed by the molecular target on which the compound is reported to act (in brackets). Red-colored boxes indicate drugs that, at the indicated concentrations, preferentially inhibited the growth of mutated cells, whereas green boxes show compounds to which mutated cells were more resistant compared with the WT counterpart. Black boxes indicate no significant difference in response between mutant and parental cells, whereas gray boxes indicate experiments not performed.

Published OnlineFirst October 9, 2013; DOI: 10.1158/1535-7163.MCT-13-0243

protein. To this aim, two *BRAF*-mutant colorectal cancer lines sensitive to proteasome inhibition (SNU-C5 and LS411N) were treated with carfilzomib and with the BRAF V600E inhibitor PLX4720, alone or in combination. Indeed, PLX4720 cotreatment impaired the response to the proteasome inhibitor and antagonism between these drugs was observed in both cell lines (Fig. 5). These findings suggest that the persistent activation of BRAF V600E signaling is required for the activity of proteasome inhibitors in *BRAF*-mutant colorectal cancer cell lines.

Finally, we tested the *in vivo* efficacy of the proteasome inhibitor carfilzomib as single agent on *BRAF*-mutant xenografts. To this aim, we used immunodeficient mice xenografted with human RKO cells. Nineteen days after cell injection, palpable tumors were present in all animals, and cohorts of mice were treated with vehicle or carfilzomib. Figure 6A shows that treatment of mice with

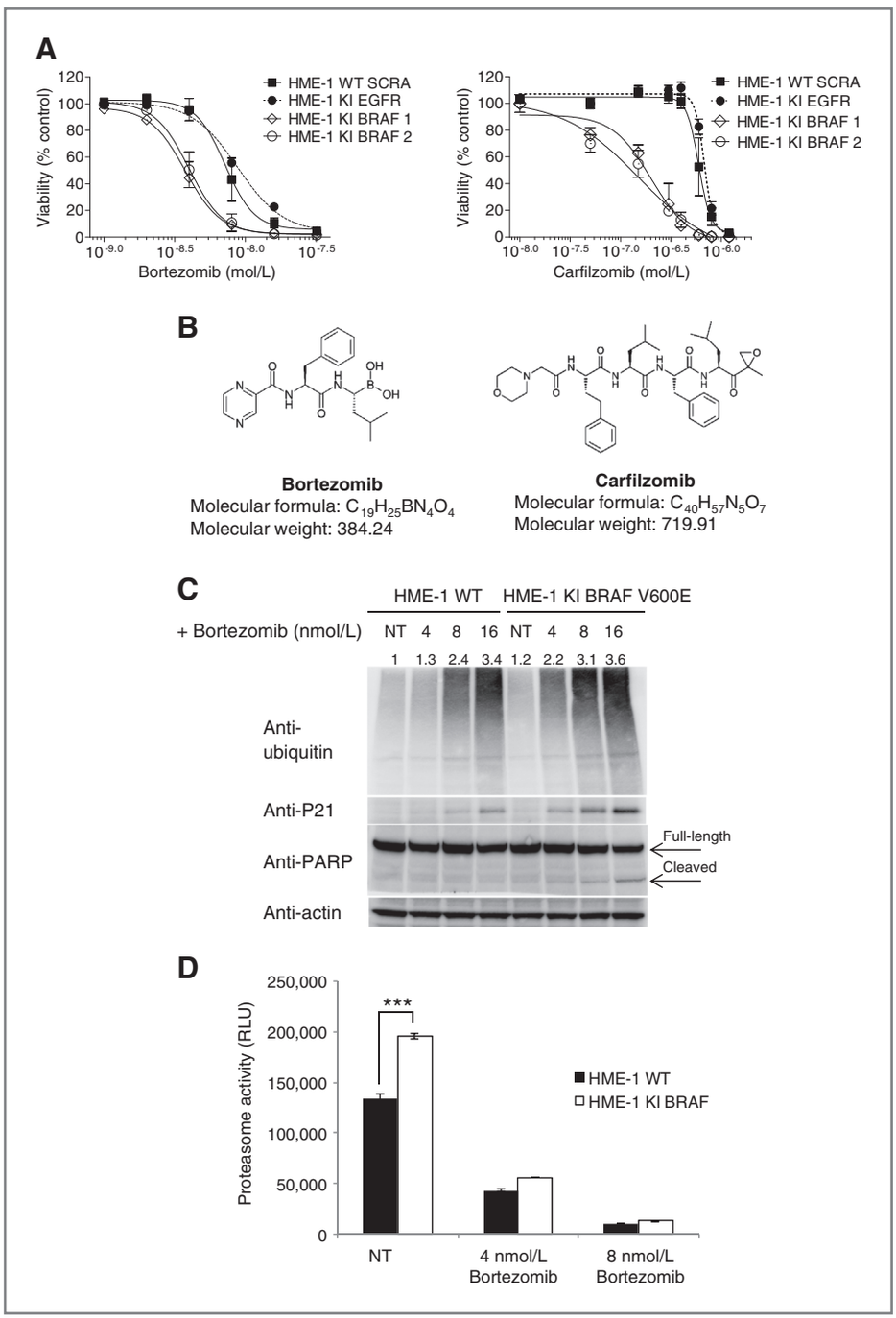

Figure 3. HME-1 clones harboring the *BRAF* V600E mutation showed increased sensitivity to proteasome inhibitors. A, effect of the proteasome inhibitors bortezomib or carfilzomib on isogenic HME-1 cells WT *BRAF* or *EGFR* mutated. Cell viability was estimated by determining ATP content in three replicate wells. Results are normalized to growth of cells treated with DMSO, and are represented as mean ± SD of at least three independent experiments. B, chemical structures, molecular formulas, and molecular weights of proteasome inhibitors bortezomib and carfilzomib. C, biochemical effects induced by treatment with increasing concentrations of bortezomib were tested by Western blot on HME-1 WT or *BRAF* KI cell lines. Ubiquitin and P21 accumulation were measured by antibodies recognizing the respective proteins, and changes in the levels of both the full-length and the cleaved form of PARP were assessed by an anti-PARP antibody. An antibody against actin was used as a loading control. Different nanomolar concentrations of the drug are reported in the top panel of the figure; densitometric quantification of the ubiquitin smears is reported above the lanes. NT, untreated controls. D, basal chymotrypsin-like proteasome activity is higher in HME-1 KI *BRAF* as compared with HME-1 WT cells, whereas titration with bortezomib reduced the activity to similar levels in the different cell lines. Twenty-four hours after seeding, cells were treated with bortezomib for 3 hours before exposure to luminogenic substrate for 15 minutes. Data are represented as mean ± SD. One KI clone is represented from two independently tested. NT, untreated controls. *P* value was determined by the Student *t* test. ***, $P < 0.001$ versus control.

Published OnlineFirst October 9, 2013; DOI: 10.1158/1535-7163.MCT-13-0243

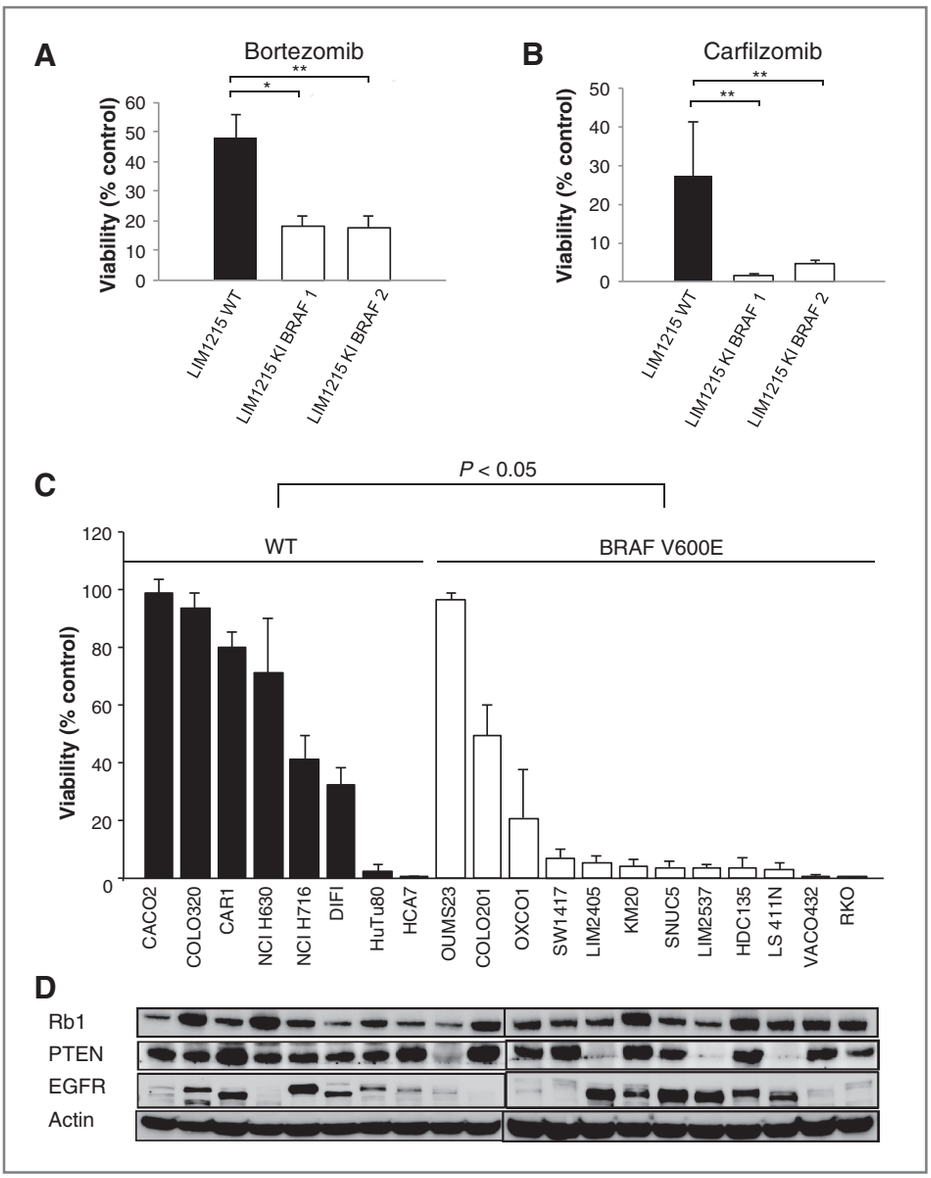

Figure 4. *BRAF*-mutant colorectal cancer lines are highly sensitive to proteasome inhibitors. The effect of the proteasome inhibitors bortezomib 40 nmol/L (A) or carfilzomib 800 nmol/L (B) on WT LIM1215 colorectal cancer cells or on two independent *BRAF* KI clones (called KI BRAF 1 and KI BRAF 2) is shown. Cell viability was estimated by determining ATP content in three replicate wells. Results are normalized to the growth of cells treated with DMSO and are represented as mean ± SEM of at least three independent experiments performed in triplicate. *P* values were determined by the Student *t* test. *, $P < 0.05$; **, $P < 0.01$ versus control. C, carfilzomib was tested on a panel of colorectal cancer cell lines WT for *BRAF* and *KRAS* (left, black columns) or harboring the *BRAF* V600E mutation (right, white columns). A single concentration of the drug was assayed on all cell lines (800 nmol/L). Cell viability was estimated by determining ATP content in three replicate wells. Results are normalized to growth of cells treated with DMSO and are represented as mean ± SD of at least three independent experiments. *, $P < 0.05$, *t* test between the viability of the two groups of cell lines. D, the expression of RB1, PTEN, or EGFR proteins was tested on the panel of colorectal cancer cell lines by Western blot. Protein lysates were loaded in the same order as indicated earlier, and incubated with anti-RB1 anti-PTEN or anti-EGFR antibodies. Actin was used as a loading control.

carfilzomib generally elicited a potent growth inhibition of RKO colorectal cancer tumors. Moreover, proteasome inhibitor promoted severe shrinkage in most of the individual treated tumors (Fig. 6B). These encouraging results support the clinical testing of carfilzomib in *BRAF*-mutant metastatic patients with colorectal cancer.

Discussion

Establishing pharmacogenomic relationships between genetic aberrations and targeted therapies is an important goal for researchers and clinicians in the era of "precision medicine". However, the presence of a single genetic lesion that is known to be a potential driver of malignant proliferation in a particular cancer does not always predict *a priori* response to treatment. Indeed, recent clinical evidence has indicated that combinations of genetic alterations within the same tumor can influence drug response (12, 14). Thus, the development of a model in which mutations can be systematically combined and tested for drug sensitivity or resistance is of increasing importance.

Several previous studies have attempted to unveil cancer pharmacogenomic relationships. Isogenic cell models able to effectively recapitulate single genetic aberrations have been employed extensively to establish binary drug–genotype associations (20, 30, 31). Nevertheless, limited efforts have been dedicated to dissect the role of combinations of mutations in determining drug response. Among these studies, it is worth mentioning the use of isogenic cell lines to evaluate the influence of *KRAS* or *TP53* status on the sensitivity to

Published OnlineFirst October 9, 2013; DOI: 10.1158/1535-7163.MCT-13-0243

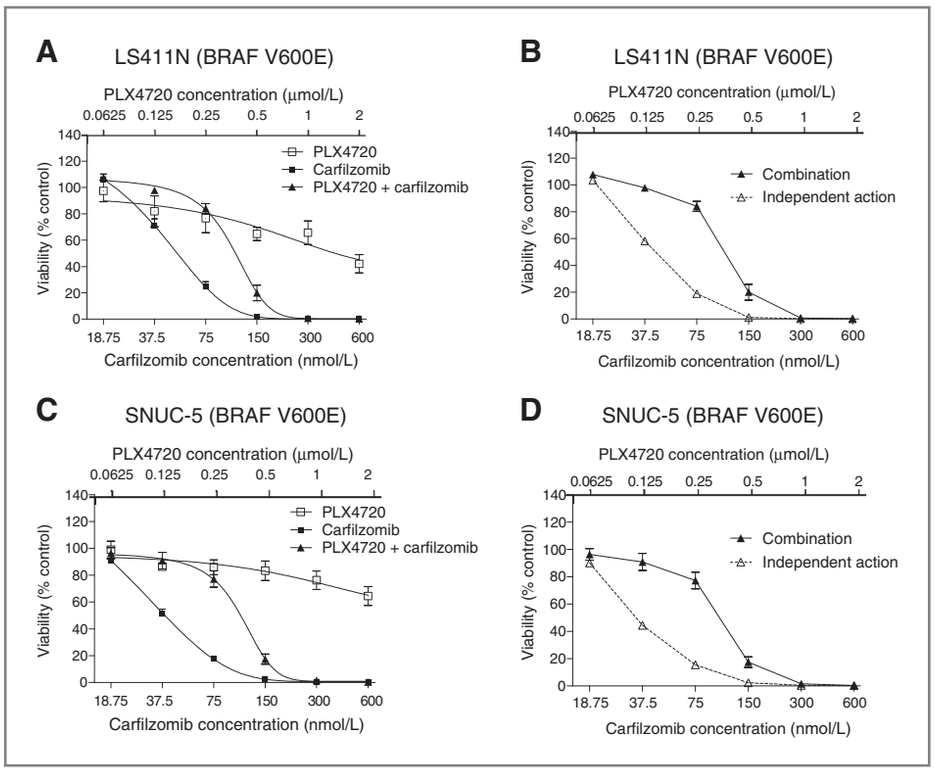

Figure 5. BRAF signaling determines vulnerability to proteasome inhibitors in *BRAF*-mutant colorectal cancer cells. The effect of multiple concentrations of carfilzomib and PLX4720, alone or in combination, was assessed on the *BRAF*-mutant cell lines LS411N (A and B) and SNUC-5 (C and D). Cell viability was determined by calculation of ATP content in triplicate in LS411N (A) or in SNUC-5 (C). Results were normalized to the growth of cells treated with DMSO, and are represented as mean ± SD of a representative experiment from a total of three. By the method of Poch and colleagues (23), the observed effect of the combination at each concentration is lower than the expected effect (independent action) for LS411N (B) and SNUC-5 (D) cell lines.

specific anticancer therapies in defined genetic backgrounds (32–35).

This report aimed to identify new pharmacogenomic relationships by screening 43 selected compounds on a panel of isogenic models harboring multiple cancer associated alterations. In comparison with previous studies, two major improvements have been implemented. First, we employed epithelial human cell models that closely recapitulated combinations of cancer mutations. Indeed, KI of nucleotide changes in oncogenes and knockdown of tumor suppressor genes were coupled to build a genetic 'matrix' in the human breast epithelial cell line HME-1 (15). The advantage of this matrix is that expression levels of mutant oncoproteins are similar to levels observed in human tumors, as they are controlled by endogenous genomic elements. Second, we screened a panel of 43 selected compounds, including a number of last generation and FDA-approved targeted therapies, to maximize the translational impact of the screening outcome.

The "Pharmarray" approach that we previously developed (20) was then applied to analyze the drug screening profiles of the combinatorial HME-1 'matrix' (15). By the use of the cell matrix, previous observations that *EGFR* KI cells show increased sensitivity to the EGFR kinase inhibitors gefitinib and erlotinib (20) were extended to novel HER-targeted agents such as vandetanib, canertinib, and lapatinib. Consistent with previous studies, this phenotype was partially rescued by the silencing of the *PTEN* tumor suppressor gene, confirming that our model system can recapitulate complex pharmacogenomic relationships found in lung tumors (12). We envision that the use of more dedicated methods of analysis of the Pharmarray data will unveil other similar interactions in which the drug response is impacted by *PTEN* or *RB1* silencing in specific KI genotypes. Indeed, those relationships might become evident by systematically analyzing drug responses normalized versus different genotypes instead of WT cells.

However, in the present work, we aimed to show novel pharmacogenomic relationships that were not significantly affected by the concomitant inactivation of the tumor suppressor genes analyzed in the matrix. Pharmarray analysis showed that the *BRAF*-mutant cells were preferentially targeted by the proteasome inhibitor bortezomib independently from the silencing of PTEN or RB1.

The genotype-specific activity of bortezomib was corroborated by the use of an irreversible proteasome inhibitor, carfilzomib, suggesting that this effect was due to target inhibition and not to peculiar pharmacologic properties of bortezomib. Interestingly, this pharmacogenomic relationship was also observed in *KRAS* G13D–mutant cells albeit less pronounced than in *BRAF* V600E cells. Our results, therefore, support claims that proteasome inhibitors, such as MG132 and bortezomib, display synthetic lethality with respect to *KRAS* mutations in cancer cells (36).

Selective targeting of *BRAF*-mutant cells by proteasome inhibitors was not affected by concomitant inactivation of *PTEN* or *RB1* tumor suppressors. This is different from what was previously reported for BRAF/MEK inhibitors

Published OnlineFirst October 9, 2013; DOI: 10.1158/1535-7163.MCT-13-0243

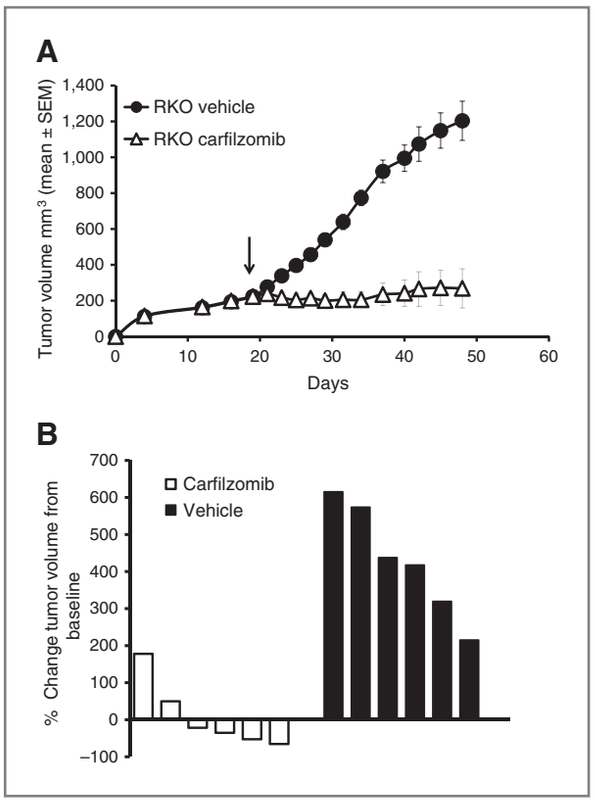

Figure 6. Carfilzomib suppresses the growth of *BRAF*-mutant RKO xenografts. A, following tumor establishment (200–250 mm^3), mice were treated with vehicle or carfilzomib i.v. at 4 mg/kg. Tumor volumes are shown as mean ± SEM ($n = 6$ mice per group). The arrow indicates the time at which treatment was started. B, waterfall plot showing the percentage change in volume for the individual tumors in each arm following 30 days of vehicle or carfilzomib treatment. Tumor volumes were normalized individually to their volume at treatment day 1.

as concomitant mutational inactivation of *PTEN* or *RB1* diminished response to those agents in melanomas harboring *BRAF* V600E (37). Therefore, targeting the proteasome may represent a valuable alternative to BRAF or MEK kinase inhibition for the treatment of *BRAF*-mutant tumors harboring *PTEN* or *RB1* alterations.

BRAF inhibitors showed poor activity also in *BRAF* mutated metastatic colorectal cancer (17, 29), and novel treatment strategies are required to improve treatment options and survival in such patients.

Although bortezomib was the first proteasome inhibitor to show antitumor activity against a variety of hematologic malignancies, it demonstrated poor efficacy as a single agent in both phase 1 and 2 trials on a broad range of solid tumors, including colorectal cancer (38–40). Carfilzomib is the first new-generation FDA-approved proteasome inhibitor. Differently from bortezomib, carfilzomib is an irreversible inhibitor, characterized by a potent and persistent proteasome inhibition and greater selectivity for the chymotrypsin-like activity of the proteasome (41). It showed antitumor activity on xenografted cancer cell lines originating from solid tumors (42). A phase 1 study of carfilzomib has shown that it is well tolerated with consecutive day dosing (43), and a phase 1b/2 study on relapsed solid tumors is ongoing [http://www.clinicaltrials.gov].

For the abovementioned reasons, we sought to confirm the preferential targeting of *BRAF*-mutant cells by carfilzomib in cancer models of colorectal cancer origin. Importantly, we demonstrated that carfilzomib preferentially inhibited the growth of mutant *BRAF* with respect to the WT colorectal cancer cell lines, corroborating the results obtained in the isogenic models. Carfilzomib exhibited a potent antineoplastic activity as single agent also *in vivo* on the RKO *BRAF*-mutant colorectal cancer cell line.

The encouraging results from preclinical trials and the findings reported in this work suggest that new-generation irreversible proteasome inhibitors may represent a valuable approach to target colorectal cancer cells harboring the *BRAF* V600E mutation.

It should be acknowledged that our screening showed exceptions to the selective targeting of *BRAF*-mutant colorectal cancer cells by carfilzomib. We believe that the characterization of those outliers is important to understand the basis of the genotype-specific inhibition by antiproteasome compounds. In addition, this approach may help in better defining the subset of patients that most likely would benefit from antiproteasome treatments because there are currently no predictive biomarkers for this class of agents.

We hypothesized that some of those exceptions may be explained by known mechanisms of resistance to BRAF inhibitors in *BRAF*-mutant colorectal cancer cells. It was shown that EGFR expression confers primary resistance to BRAF inhibition in *BRAF* V600E–mutant colorectal cancer (29). Nevertheless, EGFR expression did not correlate with sensitivity to proteasome inhibitors in our cell panel. Another hypothesis relies on the observation that *BRAF*-mutant colorectal cancer samples are frequently associated to microsatellite instable (MSI) phenotype (44). As many *BRAF*-mutant cell lines employed in the present study are MSI, including the LIM1215 KI *BRAF* isogenic models, we cannot rule out the possibility that microsatellite instability contribute together with *BRAF V600E* mutation to increase the sensitivity to proteasome inhibition.

To our knowledge, this is the first report to show that proteasome inhibition could act preferentially on cancer cells with oncogenic *BRAF*. Mechanistically, we speculate that BRAF-mutant cells may experience a nononcogenic addiction to the proteasome function because the protein degradation mediated by the ubiquitin–proteasome system is needed to counterbalance the proteotoxic stress induced by the mutant protein. Indeed, different oncogenes have been associated to proteotoxic stress responses (45) and phenomena of nononcogenic addiction to the proteasome activity have been shown also for *KRAS*-mutant cells (36, 46). The evidence that—following proteasome blockade—a higher accumulation rate of ubiquitinated proteins occurred in mutant cells with respect to the WT supports our model. Importantly, in support of our hypothesis, we also showed that the dependence from

Published OnlineFirst October 9, 2013; DOI: 10.1158/1535-7163.MCT-13-0243

proteasome function is dependent upon the persistence of BRAF V600E activity.

In conclusion, we have shown that isogenic models in the "matrix" described in this article can be exploited for synthetic lethality screenings to identify drugs that are selectively toxic for cancer cells carrying complex tumor genotypes. Indeed, this analysis led to the identification of the new, potentially relevant drug–genotype correlation between *BRAF* mutation and proteasome inhibition.

We acknowledge that combinations of multiple drugs are often needed to maximize the antitumor effect and to delay the onset of resistance (47). The next challenge of personalized medicine will be tailoring the right combinatorial therapy to the right complex tumor genotype. Indeed, approaches to perform high-throughput screenings of combinations of compounds have been published and showed remarkable results also in the analysis of *BRAF*-mutant melanoma cells (48, 49). Therefore, we envision that the screening of drug combinations on specific components of the matrix, such as genotypes harboring *BRAF* mutation, will represent a valuable strategy to unveil more effective therapy–genotype correlations.

Disclosure of Potential Conflicts of Interest

A. Bardelli has ownership interests, including patents, is a shareholder, and is a member of the Scientific Advisory Board at Horizon Discovery Ltd, United Kingdom, to which some of the cell lines described in this article have been licensed through the University of Turin. No potential conflicts of interest were disclosed by the other authors.

Authors' Contributions

Conception and design: D. Zecchin, V. Boscaro, A. Bardelli, M. Gallicchio, F. Di Nicolantonio
Development of methodology: D. Zecchin, A. Bardelli, F. Di Nicolantonio
Acquisition of data (provided animals, acquired and managed patients, provided facilities, etc.): D. Zecchin, V. Boscaro, L. Barault, M. Martini, C. Cancelliere, A. Bartolini, M. Gallicchio, F. Di Nicolantonio
Analysis and interpretation of data (e.g., statistical analysis, biostatistics, computational analysis): D. Zecchin, E. Medico, F. Di Nicolantonio
Writing, review, and/or revision of the manuscript: D. Zecchin, E. Medico, L. Barault, M. Martini, C. Cancelliere, E.H. Crowley, A. Bardelli, F. Di Nicolantonio
Administrative, technical, or material support (i.e., reporting or organizing data, constructing databases): D. Zecchin, S. Arena
Study supervision: V. Boscaro, A. Bardelli, M. Gallicchio, F. Di Nicolantonio

Grant Support

This work was financially supported by funding from the Fondazione Piemontese per la Ricerca sul Cancro ONLUS grant 'Farmacogenomica – 5 per mille 2009 MIUR' (to F. Di Nicolantonio), the AIRC (grant no. MFAG 11349 to F. Di Nicolantonio), the European Community's Seventh Framework Programme (grant no. 259015 COLTHERES), the AIRC 2010 Special Program Molecular Clinical Oncology 5 x Mille (Project no. 9970 to A. Bardelli and E. Medico), Intramural Grants Fondazione Piemontese per la Ricerca sul Cancro ONLUS (5 per mille 2008 MIUR to A. Bardelli, E. Medico, and F. Di Nicolantonio). Both D. Zecchin and L. Barault are recipients of a postdoctoral fellowship from the Fondazione Umberto Veronesi – Young Investigator Programme 2013.

The costs of publication of this article were defrayed in part by the payment of page charges. This article must therefore be hereby marked *advertisement* in accordance with 18 U.S.C. Section 1734 solely to indicate this fact.

Received April 4, 2013; revised September 18, 2013; accepted September 21, 2013; published OnlineFirst October 9, 2013.

References

1. Lynch TJ, Bell DW, Sordella R, Gurubhagavatula S, Okimoto RA, Brannigan BW, et al. Activating mutations in the epidermal growth factor receptor underlying responsiveness of non-small-cell lung cancer to gefitinib. N Engl J Med 2004;350:2129–39.
2. Paez JG, Janne PA, Lee JC, Tracy S, Greulich H, Gabriel S, et al. EGFR mutations in lung cancer: correlation with clinical response to gefitinib therapy. Science 2004;304:1497–500.
3. Pao W, Miller V, Zakowski M, Doherty J, Politi K, Sarkaria I, et al. EGF receptor gene mutations are common in lung cancers from "never smokers" and are associated with sensitivity of tumors to gefitinib and erlotinib. Proc Natl Acad Sci U S A 2004;101:13306–11.
4. Sordella R, Bell DW, Haber DA, Settleman J. Gefitinib-sensitizing EGFR mutations in lung cancer activate anti-apoptotic pathways. Science 2004;305:1163–7.
5. Vogel CL, Cobleigh MA, Tripathy D, Gutheil JC, Harris LN, Fehrenbacher L, et al. Efficacy and safety of trastuzumab as a single agent in first-line treatment of HER2-overexpressing metastatic breast cancer. J Clin Oncol 2002;20:719–26.
6. Chapman PB, Hauschild A, Robert C, Haanen JB, Ascierto P, Larkin J, et al. Improved survival with vemurafenib in melanoma with BRAF V600E mutation. N Engl J Med 2011;364:2507–16.
7. Hauschild A, Grob JJ, Demidov LV, Jouary T, Gutzmer R, Millward M, et al. Dabrafenib in BRAF-mutated metastatic melanoma: a multicentre, open-label, phase 3 randomised controlled trial. Lancet 2012;380:358–65.
8. Kwak EL, Bang YJ, Camidge DR, Shaw AT, Solomon B, Maki RG, et al. Anaplastic lymphoma kinase inhibition in non-small-cell lung cancer. N Engl J Med 2010;363:1693–703.
9. Shaw AT, Yeap BY, Solomon BJ, Riely GJ, Gainor J, Engelman JA, et al. Effect of crizotinib on overall survival in patients with advanced non-small-cell lung cancer harbouring ALK gene rearrangement: a retrospective analysis. Lancet Oncol 2011;12:1004–12.
10. Wood LD, Parsons DW, Jones S, Lin J, Sjoblom T, Leary RJ, et al. The genomic landscapes of human breast and colorectal cancers. Science 2007;318:1108–13.
11. Mellinghoff IK, Wang MY, Vivanco I, Haas-Kogan DA, Zhu S, Dia EQ, et al. Molecular determinants of the response of glioblastomas to EGFR kinase inhibitors. N Engl J Med 2005;353:2012–24.
12. Sos ML, Koker M, Weir BA, Heynck S, Rabinovsky R, Zander T, et al. PTEN loss contributes to erlotinib resistance in EGFR-mutant lung cancer by activation of Akt and EGFR. Cancer Res 2009;69:3256–61.
13. Berns K, Horlings HM, Hennessy BT, Madiredjo M, Hijmans EM, Beelen K, et al. A functional genetic approach identifies the PI3K pathway as a major determinant of trastuzumab resistance in breast cancer. Cancer Cell 2007;12:395–402.
14. Esteva FJ, Guo H, Zhang S, Santa-Maria C, Stone S, Lanchbury JS, et al. PTEN, PIK3CA, p-AKT, and p-p70S6K status: association with trastuzumab response and survival in patients with HER2-positive metastatic breast cancer. Am J Pathol 2010;177:1647–56.
15. Zecchin D, Arena S, Martini M, Sassi F, Pisacane A, Di Nicolantonio F, et al. Modeling tumor progression by the sequential introduction of genetic alterations into the genome of human normal cells. Hum Mutat 2013;34:330–7.
16. Richman SD, Seymour MT, Chambers P, Elliott F, Daly CL, Meade AM, et al. KRAS and BRAF mutations in advanced colorectal cancer are associated with poor prognosis but do not preclude benefit from oxaliplatin or irinotecan: results from the MRC FOCUS trial. J Clin Oncol 2009;27:5931–7.
17. Kopetz S, Desai J, Chan E, Hecht JR, O'Dwyer PJ, Lee RJ, et al. PLX4032 in metastatic colorectal cancer patients with mutant BRAF tumors. J Clin Oncol 28:15s, 2010 (suppl; abstr 3534).
18. Whitehead RH, Macrae FA, St John DJ, Ma J. A colon cancer cell line (LIM1215) derived from a patient with inherited nonpolyposis colorectal cancer. J Natl Cancer I 1985;74:759–65.

Published OnlineFirst October 9, 2013; DOI: 10.1158/1535-7163.MCT-13-0243

19. Zhang HH, Walker F, Kiflemariam S, Whitehead RH, Williams D, Phillips WA, et al. Selective inhibition of proliferation in colorectal carcinoma cell lines expressing mutant APC or activated B-Raf. Int J Cancer 2009;125:297–307.
20. Di Nicolantonio F, Arena S, Gallicchio M, Zecchin D, Martini M, Flonta SE, et al. Replacement of normal with mutant alleles in the genome of normal human cells unveils mutation-specific drug responses. Proc Natl Acad Sci U S A 2008;105:20864–9.
21. Zecchin D, Di Nicolantonio F. Transfection and DNA-mediated gene transfer. Methods Mol Biol 2011;731:435–50.
22. Fu L, Medico E. FLAME, a novel fuzzy clustering method for the analysis of DNA microarray data. BMC Bioinformatics 2007;8:3.
23. Poch G, Reiffenstein RJ, Kock P, Pancheva SN. Uniform characterization of potentiation in simple and complex situations when agents bind to different molecular sites. Can J Physiol Pharmacol 1995;73:1574–81.
24. Di Nicolantonio F, Martini M, Molinari F, Sartore-Bianchi A, Arena S, Saletti P, et al. Wild-type BRAF is required for response to panitumumab or cetuximab in metastatic colorectal cancer. J Clin Oncol 2008;26:5705–12.
25. Gandhi J, Zhang J, Xie Y, Soh J, Shigematsu H, Zhang W, et al. Alterations in genes of the EGFR signaling pathway and their relationship to EGFR tyrosine kinase inhibitor sensitivity in lung cancer cell lines. PLoS ONE 2009;4:e4576.
26. Jhawer M, Goel S, Wilson AJ, Montagna C, Ling YH, Byun DS, et al. PIK3CA mutation/PTEN expression status predicts response of colon cancer cells to the epidermal growth factor receptor inhibitor cetuximab. Cancer Res 2008;68:1953–61.
27. Barretina J, Caponigro G, Stransky N, Venkatesan K, Margolin AA, Kim S, et al. The Cancer Cell Line Encyclopedia enables predictive modelling of anticancer drug sensitivity. Nature 2012;483:603–7.
28. Garnett MJ, Edelman EJ, Heidorn SJ, Greenman CD, Dastur A, Lau KW, et al. Systematic identification of genomic markers of drug sensitivity in cancer cells. Nature 2012;483:570–5.
29. Prahallad A, Sun C, Huang S, Di Nicolantonio F, Salazar R, Zecchin D, et al. Unresponsiveness of colon cancer to BRAF(V600E) inhibition through feedback activation of EGFR. Nature 2012;483:100–3.
30. Li HF, Keeton A, Vitolo M, Maddox C, Rasmussen L, Hobrath J, et al. A high-throughput screen with isogenic PTEN+/+ and PTEN-/- cells identifies CID1340132 as a novel compound that induces apoptosis in PTEN and PIK3CA mutant human cancer cells. J Biomol Screen 2011;16:383–93.
31. Torrance CJ, Agrawal V, Vogelstein B, Kinzler KW. Use of isogenic human cancer cells for high-throughput screening and drug discovery. Nat Biotechnol 2001;19:940–5.
32. Dolma S, Lessnick SL, Hahn WC, Stockwell BR. Identification of genotype-selective antitumor agents using synthetic lethal chemical screening in engineered human tumor cells. Cancer Cell 2003;3:285–96.
33. Shaw AT, Winslow MM, Magendantz M, Ouyang C, Dowdle J, Subramanian A, et al. Selective killing of K-ras mutant cancer cells by small molecule inducers of oxidative stress. Proc Natl Acad Sci U S A 2011;108:8773–8.
34. Sur S, Pagliarini R, Bunz F, Rago C, Diaz LAJr., Kinzler KW, et al. A panel of isogenic human cancer cells suggests a therapeutic approach for cancers with inactivated p53. Proc Natl Acad Sci U S A 2009;106:3964–9.
35. Weiss MB, Vitolo MI, Mohseni M, Rosen DM, Denmeade SR, Park BH, et al. Deletion of p53 in human mammary epithelial cells causes chromosomal instability and altered therapeutic response. Oncogene 2010;29:4715–24.
36. Luo J, Emanuele MJ, Li D, Creighton CJ, Schlabach MR, Westbrook TF, et al. A genome-wide RNAi screen identifies multiple synthetic lethal interactions with the Ras oncogene. Cell 2009;137:835–48.
37. Xing F, Persaud Y, Pratilas CA, Taylor BS, Janakiraman M, She QB, et al. Concurrent loss of the PTEN and RB1 tumor suppressors attenuates RAF dependence in melanomas harboring (V600E)BRAF. Oncogene 2012;31:446–57.
38. Caponigro F, Lacombe D, Twelves C, Bauer J, Govaerts AS, Marreaud S, et al. An EORTC phase I study of Bortezomib in combination with oxaliplatin, leucovorin and 5-fluorouracil in patients with advanced colorectal cancer. Eur J Cancer 2009;45:48–55.
39. Caravita T, de Fabritiis P, Palumbo A, Amadori S, Boccadoro M. Bortezomib: efficacy comparisons in solid tumors and hematologic malignancies. Nat Clin Pract Oncol 2006;3:374–87.
40. Milano A, Perri F, Caponigro F. The ubiquitin-proteasome system as a molecular target in solid tumors: an update on bortezomib. Onco Targets Ther 2009;2:171–8.
41. Kuhn DJ, Chen Q, Voorhees PM, Strader JS, Shenk KD, Sun CM, et al. Potent activity of carfilzomib, a novel, irreversible inhibitor of the ubiquitin-proteasome pathway, against preclinical models of multiple myeloma. Blood 2007;110:3281–90.
42. Zang Y, Thomas SM, Chan ET, Kirk CJ, Freilino ML, DeLancey HM, et al. Carfilzomib and ONX 0912 inhibit cell survival and tumor growth of head and neck cancer and their activities are enhanced by suppression of Mcl-1 or autophagy. Clin Cancer Res 2012;18:5639–49.
43. O'Connor OA, Stewart AK, Vallone M, Molineaux CJ, Kunkel LA, Gerecitano JF, et al. A phase 1 dose escalation study of the safety and pharmacokinetics of the novel proteasome inhibitor carfilzomib (PR-171) in patients with hematologic malignancies. Clin Cancer Res 2009;15:7085–91.
44. Rajagopalan H, Bardelli A, Lengauer C, Kinzler KW, Vogelstein B, Velculescu VE. Tumorigenesis: RAF/RAS oncogenes and mismatch-repair status. Nature 2002;418:934.
45. Dai C, Whitesell L, Rogers AB, Lindquist S. Heat shock factor 1 is a powerful multifaceted modifier of carcinogenesis. Cell 2007;130:1005–18.
46. Barbie DA, Tamayo P, Boehm JS, Kim SY, Moody SE, Dunn IF, et al. Systematic RNA interference reveals that oncogenic KRAS-driven cancers require TBK1. Nature 2009;462:108–12.
47. Bernards R. A missing link in genotype-directed cancer therapy. Cell 2012;151:465–8.
48. Held MA, Langdon CG, Platt JT, Graham-Steed T, Liu Z, Chakraborty A, et al. Genotype-selective combination therapies for melanoma identified by high-throughput drug screening. Cancer Discov 2013;3:52–67.
49. Roller DG, Axelrod M, Capaldo BJ, Jensen K, Mackey A, Weber MJ, et al. Synthetic lethal screening with small-molecule inhibitors provides a pathway to rational combination therapies for melanoma. Mol Cancer Ther 2012;11:2505–15.

Supplementary Figure S1

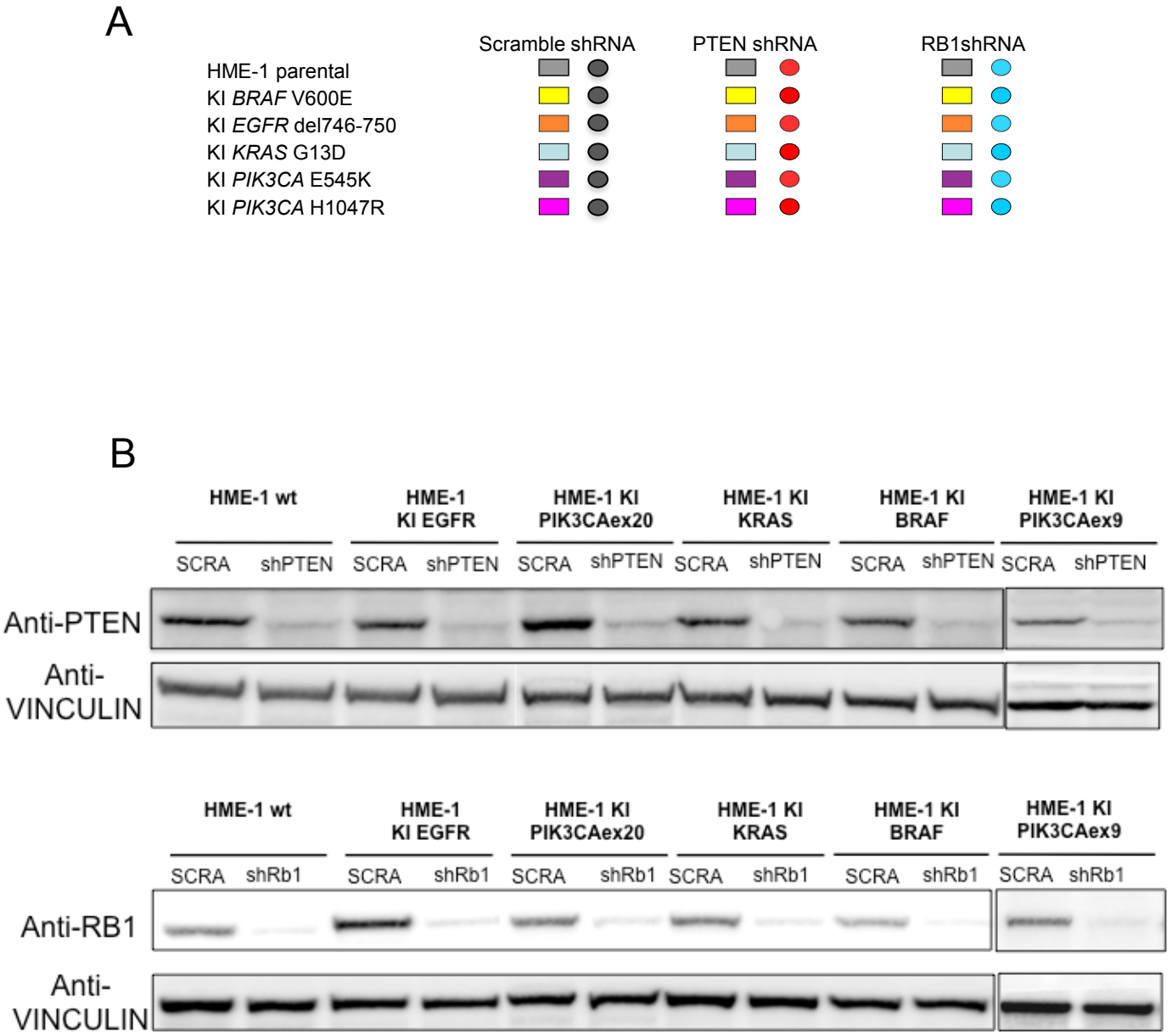

Supplementary Figure S1.
A. Genotypes included in the combinatorial genetic matrix. The chart shows how the aberrations are combined in a "matrix". Every symbol corresponds to a different KI or shRNA vector. In rows are reported the parental genetic background or the knocked-in mutations (represented by squares), in columns are reported shRNAs used to infect cells (represented by circles). HME-1 cells were used as a background
B. PTEN or RB1 were silenced by shRNA in isogenic KI cells. Knockdown levels were evaluated by western blot analysis of the target proteins. Protein levels in shRNA-infected cells were compared to those observed in cells infected with the scramble non-target shRNA (SCRA)

Supplementary Figure S2

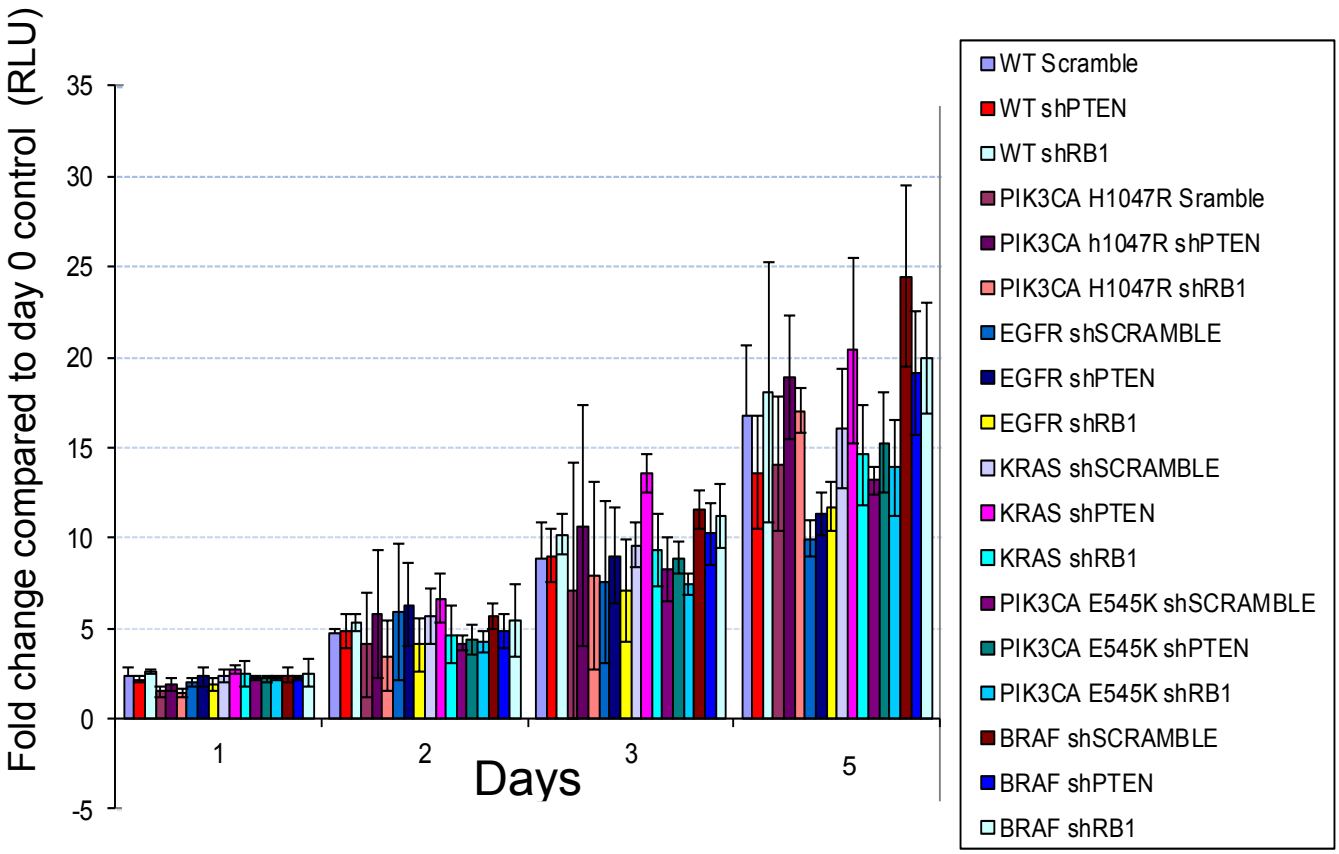

Supplementary figure S2
Comparison of the proliferation rates of the 'matrix' isogenic cellular models. Average cell number at each time point (days from seeding are reported on the x axis) was estimated by determining ATP content in quadruplicate wells. Data are represented as fold change in the mean±SD of three independent experiments. RLUs, relative light units.

Supplementary Figure S3

Supplementary figure S3
Pharmarray analysis of the isogenic cellular matrix. The cell line genotype is shown on the horizontal axis at the top of the array. Genotypes are defined according to the color code indicated in the legend. Cells carrying the indicated genetic alterations were clustered using a hierarchical un-supervised algorithm; Drugs were clustered on the vertical axis using un-supervised C-means Fuzzy algorithm. For each compound the lowest concentration used was annotated with the number 1, intermediate concentration with 2 and the highest with 3. The drug name is followed by the molecular target on which the compound is reported to act (in brackets). The bar below drug clusters indicates the probability of membership of each element to that cluster, with blue color annotating high probability and black low probability. Red-colored boxes indicate drugs that, at the indicated concentrations, preferentially inhibited the growth of mutated cells, whilst green boxes show compounds to which mutated cells were more resistant compared to the wild type counterpart. Black boxes indicate no significant difference in response between mutant and parental cells, whilst grey boxes indicate experiments not performed.

Supplementary Figure S4

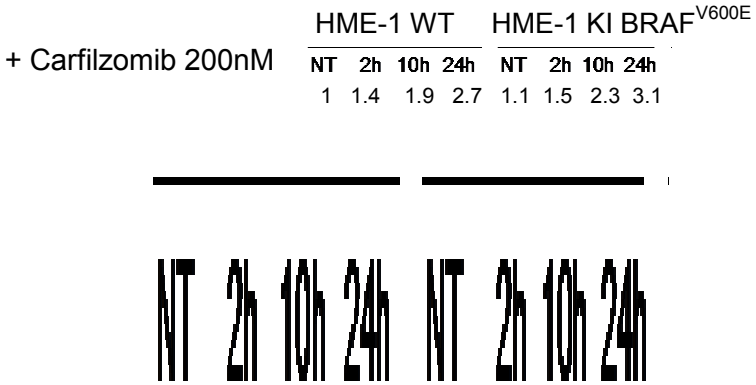

Supplementary figure S4
Biochemical effects induced by treatment with carfilzomib 200nM were tested by Western Blot on HME-1 wild type or BRAF KI. Cells were incubated with the drug for the times indicated on the upper part of the panel. Antibody against actin was used as a loading control.
Densitometric quantification of the ubiquitin smears are divided by the intensity of the respective actin bands, normalized to the sample HME-1 WT NT and reported above the lanes.
H, hours.

Supplementary table S1.
List of compounds employed in the present work. Chemical formulas, the molecular weights (MW), the solvents used for suspension, the concentrations of stock solutions, the concentrations tested in the experiments and the storage conditions used for the stock are also reported.

Drug	Formula	MW	Supplier	solvent	STOCK	Tested	Storage
Erlotinib	$C_{22}H_{23}N_3O_4$	489.5	Sequoia	DMSO	20	-7.301029995664; -6; -4.698970004	-20°C
Cetuximab	$C_{6484}H_{10042}N_{1732}O_{2023}S_{36}$	145782	Hospital Pharmacy	Ready to use	0.01372	-7.38552463391; -6.38552463391; -5.385524634	4°C
Trastuzumab	$C_{6470}H_{10012}N_{1726}O_{2013}S_{42}$	148058	Hospital Pharmacy	Ready to use	0.14184	-4.619788758288; -4.443697499233; -4.26760624	4°C
Canertinib (CI-1033)	$C_{24}H_{25}ClFN_5O_3$	485.94	AXON medchem	DMSO	20	-8.52287874528; -7.52287874528; -6.522878745	-20°C
Lapatinib (GW572016)	$C_{29}H_{26}ClFN_4O_4S$	581.06	Sequoia	DMSO	20	-7; -6; -5	-20°C
Vandetanib (ZD6474)	$C_{22}H_{24}BrFN_4O_2$	475.36	Sequoia	DMSO	20	-6.52287874528; -5.920818753952; -5.318758763	-20°C
Sunitinib	$C_{22}H_{27}FN_4O_2 \cdot C4H6O5$	532.5	Sequoia	H2O	20	-5.823908740944; -5.346787486225; -4.869666232	-20°C
Sorafenib	C21H16ClF3N4O3·C7H8O3S	637	Sequoia	DMSO	20	-6; -5.69897000434; -5.397940009	-20°C
Vatalanib	C20H15ClN4 · 2HCl	419.7	ChemieTek	H2O	20	-5.301029995664; -4.698970004336; -4.096910013	-20°C
Cediranib	C25H27FN4O3	450.51	Selleck	DMSO	10	-5.698970004336; -5.221848749616; -4.744727495	-20°C
NVP-AEW541	C27H29N5O	439.55	Selleck	DMSO	10	-6.602059991328; -6.124938736608; -5.647817482	-20°C
BMS-536924	C25H26ClN5O3	479.96	Selleck	DMSO	20	-6.301029995664; -5.823908740944; -5.346787486	-20°C
PHA-665752	$C_{32}H_{34}Cl_2N_4O_4S$	641.61	Tocris	DMSO	20	-5.647817481889; -5.471726222833; -5.295634964	-20°C
L744832	C26H45N3O6S2·2HCl	632.7	Alexis	DMSO	20	-6; -5; -4	-20°C
PLX4720	C17H14ClF2N2O3S	413.83	Selleck	DMSO	50	-5.49485002168; -4.795880017344; -4.096910013	-20°C
AZD6244 (selumetinib; ARRY-142886)	C17H15BrClFN4O3	457.69	Selleck	DMSO	20	-6.698970004336; -5.397940008672; -4.096910013	-20°C
Bosutinib	$C_{26}H_{29}Cl_2N_5O_3$	530.4	Sequoia	DMSO	10	-6.455931955649; -5.756961951314; -5.057991947	-20°C
Saracatinib (AZD0530)	$C_{27}H_{32}ClN5O5$	542.03	Sequoia	DMSO	20	-6.301029995664; -5.823908740944; -5.346787486	-20°C
NVP-BEZ235	C30H23N5O	469.55	AXON Medchem	DMSO	5	-8.397940008672; -7.397940008672; -6.397940009	-20°C
GDC-0941	C23H27N7O3S2·2CH3SO3H	705.83	AXON Medchem	DMSO	20	-6.602059991328; -5.301029995664; -4	-20°C
XL-765	C31H29N5O6S	599.66	Selleck	DMSO	10	-5.698970004336; -5.221848749616; -4.744727495	-20°C
						-6.301029995664;	

Drug	Formula	MW	Supplier	solvent	STOCK	Tested	Storage
Perifosine	C25H53NO4P	462.66	Selleck	Water	20	-5.698970004336; -5.096910013	-20°C
MK-2206	$C_{25}H_{23}Cl2N5O$	480.39	Selleck	DMSO	20	-6.602059991328; -5.602059991328; -4.602059991	-20°C
Everolimus	C53H83NO14	958.22	Sigma	DMSO	20	-11.60205999133; -8.602059991328; -5.602059991	-80°C
17-AAG	C31H43N3O8	585.7	ChemieTek	DMSO	2	-7.397940008672; -6.698970004336; -6	-20°C
Bortezomib	C19H25BN4O4	384.24	Sequoia	DMSO	20	-8.647817481889; -8.346787486225; -8.045757491	-20°C
NVP TAE 684	C30H40ClN7O3S	614.22	AXON Medchem	DMSO	20	-6; -5.52287874528; -5.045757491	-20°C
Valproic Acid	C8H15NaO2	166.2	LKT Laboratories	Medium	200	-3.249491605149; -2.64743161382; -2.045371622	Prepare before using
Vorinostat (SAHA)	C14H20N2O3	264.3	Selleck	DMSO	20	-7.04575749056; -6.04575749056; -5.045757491	-20°C
Decitabine	$C_8H_{12}N_4O_4$	228.21	Sequoia	DMSO	20	-8; -6; -4;	-20°C
VX-680	$C_{23}H28N8OS$	464.59	Sequoia	DMSO	10	-9.301029995664; -7.301029995664; -5.301029995664	-20°C
BI-2536	C28H39N7O3	521.66	AXON Medchem	DMSO	10	-8; -7; -6	-20°C
GW 843682X	$C_{22}H_{18}F_3N_3O_4S$	477.46	AXON Medchem	DMSO	20	-6.096910013008; -5.096910013008; -4.096910013	-20°C
STF-62247	C15H13N3S	267.35	Selleck	DMSO	20	-5.790484985457; -4.790484985457; -3.790484985	-20°C
Obatoclax	C20H19N3O·CH4O3S	413.49	Cayman Chemicals	DMSO	20	-7.397940008672; -6.698970004336; -6	-20°C
Elesclomol	C19H20N4O2S2	400.5	Selleck	DMSO	20	-9.903089986992; -8.602059991328; -7.301029996	-20°C
Olaparib (AZD2281)	C24H23FN4O3	435.08	Selleck	DMSO	20	-7; -6; -5	-20°C
Thalidomide	C13H10N2O4	258.2	LKT Laboratories	DMSO	0.7776	-4.841637507905; -4.364516253185; -3.887394998465	Prepare before using
Lenalidomide	C13H13N3O3	259.26	Selleck	DMSO	20	-4.091514981121; -3.614393726402; -3.137272472	-20°C
Indomethacin	C19H16ClNO4	357.7	Sigma	DMSO	200	-5.356547323514; -4.356547323514; -3.356547324	-20°C
OSU-03012	$C_{26}H_{19}F_3N_4O$	460.5	Echelon	DMSO	10	-7; -6.301029995664; -5.602059991	-20°C
Atorvastatin	$C_{66}H_{68}CaF_2N_4O_{10}$	1153.6	SRP	MeOH	10	-6.45593195565; -5.853871964322; -5.251811973	Prepare before using
Rosuvastatin	$(C_{22}H_{27}FN_3O_6S)2Ca$	1001.1	SRP	MeOH	25	-5.823908740944; -5.221848749616; -4.619788758	Prepare before using
Metformin	$C_4H_{11}N_5·HCl$	165.62	Sigma	Medium	200	-2.82390874094; -2.221848749616; -1.619788758	Prepare before using

Supplementary Table S2.
List of t-tests p values comparing the responses of the different mutant cell lines to a given drug concentration with the response of the WT Scramble control cells. The genotypes of the cell lines are listed on the vertical axis and they are highlighted with different colors according to the KI genotype. Drugs are listed on the horizontal axis. For each compound the lowest concentration used was annotated with the number 1, the median concentration with 2 and the highest with 3. Cells reporting p values lower than 0.05 are highlighted in red.

Drug Name	Olaparib	Olaparib	Olaparib	Elesclomol	Elesclomol	Elesclomol	MK-2206	MK-2206	MK-2206	Lenalidomide	Lenalidomide	Lenalidomide	Metformin	Metformin	Metformin	GW843682X	GW843682X	GW843682X
Conc	**1**	**2**	**3**	**1**	**2**	**3**	**1**	**2**	**3**	**1**	**2**	**3**	**1**	**2**	**3**	**1**	**2**	**3**
Rb180210.17	0.018	0.113	0.480	0.492	0.456	0.658	0.589	0.550	0.509	0.369	0.659	0.302	0.082	0.111	0.055	0.197	0.091	0.118
PTEN80210.1	0.013	0.002	0.050	0.047	0.714	0.645	0.369	0.725	0.458	0.872	0.385	0.570	0.679	0.919	0.259	0.116	0.418	0.391
PI3Kex9-1 SCRAMBLE	0.772	0.192	0.109	0.239	0.000	0.000	0.114	0.037	0.255	0.418	0.653	0.496	0.124	0.040	0.001	0.000	0.010	0.158
PI3Kex9-2 SCRAMBLE	0.362	0.242	0.240	0.389	0.019	0.031	0.042	0.050	0.865	0.356	0.739	0.100	0.713	0.083	0.046	0.032	0.146	0.505
PI3Kex20-1 SCRAMBLE	0.005	0.102	0.551	0.269	0.285	0.332	0.341	0.223	0.033	0.758	0.423	0.966	0.852	0.468	0.267	0.819	0.528	0.612
PI3Kex9-1+Rb1	0.427	0.010	0.045	0.214	0.001	0.000	0.384	0.147	0.096	0.379	0.812	0.110	0.089	0.060	0.251	0.001	0.060	0.165
PI3Kex9-2+Rb1	0.276	0.084	0.118	0.341	0.001	0.000	0.579	0.096	0.270	0.046	0.972	0.009	0.002	0.204	0.584	0.021	0.013	0.291
PI3Kex20-1+Rb1	0.369	0.320	0.700	0.619	0.757	0.972	0.590	0.145	0.048	0.799	0.031	0.000	0.022	0.005	0.275	0.054	0.008	0.041
PI3Kex9-1+PTEN	0.363	0.024	0.245	0.566	0.000	0.000	0.723	0.173	0.048	0.337	0.528	0.591	0.605	0.374	0.007	0.114	0.022	0.064
PI3Kex9-2+PTEN	0.399	0.000	0.084	0.379	0.000	0.000	0.241	0.040	0.075	0.236	0.264	0.406	0.085	0.425	0.017	0.000	0.008	0.664
PI3Kex20-1+PTEN	0.003	0.295	0.979	0.514	0.031	0.151	0.529	0.087	0.001	0.734	0.471	0.018	0.208	0.316	0.029	0.543	0.611	0.313
KRAS 1 SCRAMBLE	0.642	0.312	0.445	0.296	0.002	0.021	0.724	0.873	0.411	0.173	0.104	0.008	0.023	0.024	0.099	0.002	0.000	0.000
KRAS 2 SCRAMBLE	0.107	0.062	0.019	0.854	0.692	0.356	0.339	0.581	0.165	0.097	0.598	0.605	0.005	0.000	0.002	0.000	0.000	0.438
KRAS 1 Rb1	0.597	0.628	0.994	0.900	0.000	0.002	0.612	0.236	0.669	0.247	0.184	0.103	0.056	0.033	0.113	0.001	0.001	0.000
KRAS 2 Rb1	0.829	0.676	0.482	0.072	0.013	0.010	0.408	0.430	0.681	0.362	0.685	0.052	0.190	0.009	0.027	0.208	0.180	0.223
KRAS 1 PTEN	0.459	0.505	0.836	0.958	0.000	0.010	0.826	0.937	0.909	0.091	0.350	0.136	0.249	0.110	0.003	0.021	0.042	0.011
KRAS 2 PTEN	0.930	0.829	0.428	0.518	0.051	0.108	0.223	0.536	0.768	0.483	0.661	0.324	0.549	0.030	0.001	0.111	0.151	0.095
EGFR 1 SCRAMBLE	ND	ND	ND	0.128	0.000	0.007	ND	0.071	ND	0.810	0.598	0.010	0.728	0.232	0.044	ND	ND	0.023
EGFR 2 SCRAMBLE	ND	ND	ND	0.490	0.000	0.000	0.318	0.165	0.040	0.297	0.558	0.057	0.399	0.038	0.001	0.032	0.002	0.174
EGFR 1 Rb1	ND	ND	ND	0.800	0.000	0.003	ND	0.178	ND	0.712	0.842	0.013	0.031	0.222	0.106	ND	ND	0.032
EGFR 2 Rb1	ND	ND	ND	0.569	0.000	0.000	0.205	0.337	0.066	0.496	0.317	0.375	0.052	0.003	0.051	0.000	0.000	0.037
EGFR 1 PTEN	ND	ND	ND	0.061	0.005	0.000	ND	0.167	ND	0.940	0.645	0.000	0.026	0.000	0.177	ND	ND	0.000
EGFR 2 PTEN	ND	ND	ND	0.217	0.000	0.000	0.000	0.208	0.233	0.145	ND	ND	0.664	0.917	0.494	ND	ND	0.679
BRAF 1 SCRAMBLE	0.355	0.502	0.099	0.864	0.000	0.000	0.820	0.557	0.635	0.545	0.048	0.005	0.320	0.039	0.000	0.266	0.289	0.656
BRAF 2 SCRAMBLE	0.134	0.008	0.103	0.274	0.132	0.000	0.967	0.485	0.435	0.470	0.961	0.332	0.133	0.027	0.189	0.049	0.011	0.019
BRAF 1 Rb1	ND	ND	ND	0.034	0.002	0.000	0.561	0.772	0.885	0.897	0.447	0.462	0.706	0.307	0.000	0.155	0.159	0.476
BRAF 2 Rb1	ND	ND	ND	0.609	0.124	0.002	0.781	0.816	0.613	0.988	0.975	0.585	0.250	0.079	0.432	0.026	0.002	0.000
BRAF 1 PTEN	0.168	0.020	0.357	0.407	0.019	0.114	0.097	0.016	0.004	0.891	0.006	0.000	0.125	0.940	0.000	0.914	0.367	0.603
BRAF 2 PTEN	0.000	0.005	0.800	0.179	0.167	0.805	0.244	0.104	0.485	0.030	0.832	0.608	0.370	0.307	0.408	0.045	0.011	0.005

OSU-03012	OSU-03012	OSU-03012	NVP-AEW541	NVP-AEW541	NVP-AEW541	Canertinib	Canertinib	Canertinib	STF-62247	STF-62247	STF-62247	BMS-536924	BMS-536924	BMS-536924	XL-765	XL-765	XL-765	Obatoclax	Obatoclax
1	**2**	**3**	**1**	**2**	**3**	**1**	**2**	**3**	**1**	**2**	**3**	**1**	**2**	**3**	**1**	**2**	**3**	**1**	**2**
0.481	0.885	0.694	0.821	0.786	0.592	0.714	0.703	0.936	0.233	0.426	0.577	0.979	0.420	0.031	0.110	0.478	0.175	0.808	0.279
0.488	0.385	0.984	0.413	0.581	0.655	0.742	0.608	0.138	0.644	0.098	0.199	0.772	0.851	0.940	0.305	0.925	0.941	0.504	0.600
0.454	0.865	0.292	0.960	0.077	0.002	0.162	0.139	0.028	0.003	0.361	0.054	0.049	0.061	0.040	0.311	0.493	0.388	0.788	0.133
0.118	0.001	0.611	0.877	0.999	0.317	0.006	0.003	0.000	0.452	0.837	0.028	0.095	0.038	0.002	0.953	0.158	0.805	0.913	0.110
0.614	0.220	0.082	0.945	0.853	0.231	0.477	0.572	0.210	0.018	0.449	0.514	0.004	0.003	0.022	0.274	0.101	0.059	0.149	0.117
0.528	0.642	0.114	0.644	0.178	0.000	0.601	0.280	0.202	0.835	0.231	0.068	0.215	0.133	0.034	0.338	0.420	0.515	0.568	0.516
0.203	0.439	0.798	0.373	0.632	0.253	0.070	0.000	0.009	0.591	0.024	0.285	0.029	0.004	0.000	0.408	0.110	0.987	0.044	0.316
0.425	0.849	0.070	0.204	0.401	0.861	0.849	0.042	0.009	0.117	0.683	0.210	0.052	0.065	0.017	0.965	0.715	0.835	0.815	0.331
0.546	0.092	0.246	0.367	0.169	0.000	0.132	0.028	0.020	0.812	0.007	0.125	0.111	0.104	0.062	0.342	0.337	0.746	0.737	0.017
0.200	0.304	0.506	0.217	0.303	0.020	0.002	0.000	0.033	0.392	0.212	0.419	0.064	0.040	0.015	0.762	0.195	0.837	0.146	0.048
0.894	0.998	0.066	0.962	0.543	0.857	0.177	0.000	0.000	0.000	0.179	0.480	0.611	0.415	0.290	0.681	0.031	0.073	ND	ND
0.109	0.426	0.941	0.680	0.077	0.066	0.169	0.000	0.000	0.187	0.705	0.000	0.906	0.747	0.044	0.839	0.996	0.561	0.753	0.783
0.823	0.661	0.604	0.627	0.425	0.133	0.037	0.000	0.003	0.625	0.197	0.029	0.037	0.012	0.047	0.100	0.297	0.149	0.602	0.948
0.363	0.816	0.672	0.952	0.315	0.115	0.367	0.001	0.000	0.511	0.345	0.000	0.619	0.185	0.045	0.434	0.930	0.072	0.687	0.657
0.432	0.442	0.568	0.501	0.844	0.308	0.147	0.000	0.000	0.164	0.012	0.002	0.740	0.586	0.025	0.035	0.522	0.194	0.699	0.676
0.253	0.593	0.066	0.288	0.003	0.000	#DIV/0!	0.000	0.000	0.720	0.145	0.002	0.937	0.924	0.036	0.861	0.764	0.149	0.954	0.766
0.347	0.134	0.816	0.235	0.166	0.001	0.218	0.000	0.000	0.305	0.210	0.007	0.254	0.998	0.005	0.124	0.430	0.181	0.712	0.925
0.893	0.024	0.939	0.389	ND	ND	ND	0.000	ND	ND	0.259	0.059	ND	ND	ND	0.000	0.000	0.002	0.070	ND
0.148	0.007	0.065	0.186	0.013	0.063	0.142	0.000	0.001	0.015	0.767	0.271	0.558	0.799	0.846	0.561	0.347	0.448	0.179	0.002
0.030	0.065	0.118	0.970	ND	ND	ND	0.001	ND	ND	0.429	0.163	ND	ND	ND	0.288	0.090	0.340	0.077	ND
0.643	0.001	0.124	0.068	0.007	0.024	0.008	0.000	0.002	0.011	0.862	1.000	0.494	0.556	0.490	0.858	0.433	0.283	0.400	0.004
0.494	0.031	0.069	0.531	ND	ND	ND	0.000	ND	ND	0.148	0.038	ND	ND	ND	0.321	0.049	0.004	0.011	ND
0.379	0.093	0.064	ND	ND	ND	0.669	0.250	ND	0.219	0.409	0.563	ND	ND	ND	0.346	0.212	0.621	0.902	0.005
0.643	0.417	0.617	0.241	0.297	0.001	0.407	0.001	0.000	0.174	0.758	0.100	0.029	0.020	0.005	0.827	0.244	0.245	0.789	0.094
0.248	0.091	0.458	0.324	0.960	0.405	0.108	0.001	0.000	0.175	0.779	0.016	0.719	0.480	0.857	0.838	0.576	0.503	0.382	0.775
0.416	0.950	0.588	0.000	0.007	0.000	0.251	0.000	0.000	0.246	0.488	0.003	0.099	0.125	0.006	0.967	0.333	0.722	0.672	0.261
0.730	0.025	0.996	0.545	1.000	0.476	0.009	0.002	0.002	0.122	0.716	0.010	0.104	0.885	0.323	0.600	0.544	0.655	0.358	0.541
0.686	0.130	0.312	0.931	0.539	0.023	0.433	0.000	0.000	0.620	0.184	0.012	0.177	0.300	0.000	0.810	0.270	0.197	0.873	0.054
0.448	0.371	0.386	0.823	0.519	0.445	0.111	0.000	0.000	0.422	0.940	0.000	0.057	0.024	0.136	0.490	0.530	0.483	0.526	0.275

Obatoclax 3	BI-2536 1	BI-2536 2	BI-2536 3	Decitabine 1	Decitabine 2	Decitabine 3	SAHA 1	SAHA 2	SAHA 3	Valproic Acid 1	Valproic Acid 2	Valproic Acid 3	Cediranib 1	Cediranib 2	Cediranib 3	Vatalanib 1	Vatalanib 2	Vatalanib 3	NVP TAE 684 1
0.375	0.856	0.499	0.656	0.650	0.827	0.840	0.891	0.840	0.537	0.157	0.798	0.920	0.572	0.837	0.851	0.888	0.216	0.081	0.554
0.487	0.596	0.495	0.146	0.834	0.517	0.715	0.252	0.465	0.553	0.184	0.628	0.938	0.882	0.697	0.735	0.846	0.235	0.177	0.914
0.199	0.599	0.365	0.453	0.013	0.046	0.274	0.149	0.186	0.817	0.607	0.583	0.114	0.315	0.658	0.092	0.474	0.820	0.000	0.079
0.280	0.362	0.710	0.095	0.054	0.509	0.439	0.366	0.491	0.388	0.767	0.976	0.184	0.510	0.656	0.000	0.098	0.652	0.127	0.043
0.363	0.415	0.649	0.004	0.388	0.507	0.694	0.470	0.524	0.329	0.569	0.278	0.486	0.423	0.977	0.002	0.378	0.696	0.244	0.544
0.484	0.861	0.922	0.750	0.765	0.054	0.009	0.234	0.294	0.541	0.353	0.811	0.095	0.765	0.455	0.059	0.336	0.760	0.117	0.142
0.434	0.597	0.737	0.104	0.775	0.287	0.308	0.184	0.421	0.964	0.069	0.704	0.083	0.843	0.674	0.000	0.302	0.225	0.001	0.075
0.329	0.274	0.989	0.435	0.382	0.390	0.745	0.880	0.655	0.779	0.917	0.742	0.675	0.385	0.632	0.684	0.682	0.026	0.000	0.643
0.150	0.685	0.682	0.610	0.971	0.143	0.012	0.498	0.724	0.305	0.178	0.220	0.093	0.390	0.375	0.000	0.699	0.521	0.776	0.198
0.201	0.422	0.814	0.231	0.171	0.538	0.876	0.335	0.871	0.887	0.194	0.785	0.091	0.922	0.834	0.000	0.465	0.567	0.729	0.120
ND	0.097	0.074	0.886	0.466	0.014	0.090	0.164	0.163	0.374	0.204	0.072	0.060	0.609	0.346	0.809	0.907	0.024	0.949	0.763
0.794	0.273	0.006	0.020	0.564	0.231	0.398	0.129	0.161	0.729	0.382	0.190	0.054	0.201	0.443	0.024	0.290	0.169	0.369	0.761
0.351	0.524	0.000	0.102	0.230	0.973	0.340	0.991	0.104	0.242	0.877	0.124	0.077	0.725	0.350	0.649	0.344	0.865	0.866	0.921
0.722	0.381	0.044	0.054	0.183	0.266	0.633	0.948	0.352	0.602	0.156	0.158	0.072	0.857	0.430	0.014	0.506	0.446	0.275	0.619
0.810	0.769	0.006	0.404	0.238	0.020	0.226	0.366	0.682	0.656	0.300	0.165	0.167	0.456	0.727	0.452	0.892	0.924	0.573	0.164
0.888	0.357	0.024	0.218	0.709	0.634	0.725	0.711	0.389	0.027	0.306	0.063	0.052	0.879	0.661	0.008	0.432	0.624	0.910	0.691
0.197	0.624	0.002	0.311	0.566	0.783	0.165	0.131	0.916	0.053	0.002	0.029	0.193	0.540	0.924	0.673	0.402	0.974	0.311	0.919
0.060	0.054	ND	0.662	0.479	0.049	0.174	0.128	0.079	0.332	0.719	0.053	0.562	ND	ND	ND	0.053	0.091	0.000	0.205
0.040	0.054	0.010	0.004	0.051	0.000	0.014	0.271	0.098	0.000	0.221	0.062	0.082	0.540	0.106	0.119	0.262	0.205	0.358	0.423
0.032	0.095	ND	0.872	0.678	0.516	0.868	0.161	0.030	0.411	0.065	0.591	0.603	ND	ND	ND	0.027	0.035	0.005	0.381
0.210	0.799	0.004	0.000	0.146	0.001	0.010	0.058	0.000	0.012	0.019	0.047	0.053	0.457	0.964	0.003	0.371	0.206	0.207	0.347
0.134	0.286	ND	0.024	0.774	0.948	0.593	0.069	0.000	0.224	0.104	0.227	0.239	ND	ND	ND	0.014	0.062	0.003	0.463
0.090	0.857	0.391	ND	0.818	0.259	0.036	0.221	0.001	0.111	0.416	0.028	0.106	ND	0.555	0.934	0.648	0.962	0.841	0.316
0.755	0.059	0.629	0.029	0.067	0.080	0.513	0.834	0.104	0.001	0.272	0.891	0.672	0.658	0.893	0.556	0.901	0.481	0.684	0.880
0.342	0.829	0.016	0.958	0.375	0.114	0.047	0.276	0.053	0.240	0.699	0.460	0.298	0.964	0.064	0.324	0.090	0.324	0.272	0.907
0.809	0.459	0.044	0.216	0.102	0.370	0.816	0.158	0.021	0.184	0.436	0.780	0.993	0.772	0.896	0.090	0.173	0.002	0.369	0.121
0.588	0.957	0.028	0.396	0.706	0.203	0.169	0.631	0.162	0.462	0.659	0.696	0.538	0.183	0.099	0.603	0.318	0.280	0.140	0.744
0.127	0.212	0.502	0.700	0.018	0.603	0.534	0.151	0.125	0.099	0.713	0.615	0.617	0.072	0.792	0.348	0.190	0.491	0.544	0.928
0.805	0.644	0.001	0.000	0.456	0.067	0.197	0.266	0.153	0.034	0.668	0.143	0.265	0.470	0.340	0.308	0.612	0.446	0.616	0.688

NVP TAE 684 2	NVP TAE 684 3	saracatinib 1	saracatinib 2	saracatinib 3	L744832 1	L744832 2	L744832 3	GDC-0941 1	GDC-0941 2	GDC-0941 3	NVP-BEZ235 1	NVP-BEZ235 2	NVP-BEZ235 3	Perifosine 1	Perifosine 2	Perifosine 3	Bosutinib 1	Bosutinib 2	Bosutinib 3
0.627	0.899	0.026	0.134	0.002	0.997	0.282	0.790	0.723	0.786	0.732	0.286	0.736	0.870	0.784	0.590	0.820	0.846	0.730	0.376
0.956	0.856	0.062	0.015	0.461	0.099	0.053	0.392	0.350	0.514	1.000	0.396	0.737	0.907	0.861	0.081	0.780	0.540	0.029	0.164
0.010	0.016	0.153	0.000	0.001	0.041	0.484	0.317	0.181	0.011	0.817	0.163	0.669	0.403	0.616	0.722	0.479	0.355	0.004	0.000
0.000	0.038	0.003	0.037	0.000	0.000	0.000	0.885	0.780	0.820	0.007	0.351	0.447	0.080	0.790	0.298	0.054	0.021	0.002	0.000
0.017	0.075	0.007	0.021	0.004	0.376	0.349	0.001	#DIV/0!	#DIV/0!	#DIV/0!	0.171	0.200	0.935	0.708	0.267	0.266	0.008	0.031	0.000
0.058	0.024	0.615	0.000	0.029	0.095	0.370	0.782	0.047	0.000	0.262	0.502	0.972	0.392	0.987	0.908	0.485	0.166	0.002	0.000
0.000	0.022	0.007	0.001	0.009	0.003	0.000	0.776	0.004	0.268	0.109	0.484	0.436	0.004	0.779	0.604	0.046	0.003	0.000	0.000
0.086	0.040	0.006	0.001	0.001	0.702	0.295	0.003	ND	ND	ND	0.158	0.947	0.884	0.576	0.793	0.628	0.011	0.006	0.005
0.044	0.002	0.875	0.173	0.047	0.259	0.652	0.398	0.008	0.024	0.594	0.415	0.610	0.372	0.568	0.555	0.482	0.005	0.001	0.000
0.007	0.013	0.017	0.003	0.000	0.000	0.012	0.865	0.001	0.162	0.959	0.192	0.836	0.097	0.736	0.949	0.481	0.083	0.098	0.000
0.480	0.332	0.546	0.258	0.071	0.000	0.000	0.554	ND	ND	ND	0.851	0.126	0.939	0.124	0.083	0.459	0.003	0.000	0.002
0.812	0.893	0.000	0.023	0.036	0.062	0.044	0.000	0.519	0.491	0.039	0.059	0.764	0.217	0.755	0.748	0.642	0.110	0.044	0.101
0.410	0.061	0.029	0.064	0.019	0.100	0.116	0.008	0.055	0.051	0.001	0.621	0.928	0.078	0.047	0.002	0.045	0.000	0.000	0.055
0.800	0.867	0.000	0.003	0.000	0.056	0.052	0.000	0.981	0.465	0.001	0.469	0.300	0.320	0.702	0.872	0.389	0.158	0.046	0.002
0.782	0.660	0.000	0.003	0.000	0.303	0.559	0.010	0.208	0.232	0.003	0.929	0.933	0.497	0.058	0.037	0.063	0.001	0.004	0.000
0.283	0.731	0.000	0.086	0.082	0.299	0.354	0.000	0.646	0.976	0.763	0.510	0.854	0.008	0.437	0.832	0.821	0.286	0.401	0.000
0.169	0.253	0.008	0.043	0.043	0.893	0.673	0.002	0.481	0.610	0.013	0.692	0.519	0.461	0.153	0.000	0.073	0.002	0.004	0.000
ND	0.709	0.683	ND	0.002	0.000	0.057	0.006	0.318	0.127	0.000	ND	0.174	0.104	ND	0.055	0.895	0.019	0.032	0.928
0.499	0.175	0.215	0.036	0.008	0.010	0.013	0.914	0.270	0.087	0.421	0.074	0.361	0.011	0.740	0.284	0.067	0.083	0.000	0.001
ND	0.342	0.765	ND	0.478	0.275	0.118	0.001	0.325	0.114	0.000	ND	0.175	0.055	ND	0.123	0.659	0.967	0.431	0.958
0.457	0.214	0.048	0.470	0.856	0.006	0.000	0.195	0.000	0.021	0.130	0.730	0.282	0.006	0.842	0.008	0.056	0.143	0.001	0.000
ND	0.523	0.312	ND	0.000	0.142	0.008	0.003	0.648	0.264	0.000	ND	0.178	0.012	ND	0.001	0.427	0.003	0.001	0.420
0.382	0.530	0.615	0.802	0.258	ND	ND	ND	0.321	0.231	0.689	ND	0.562	0.121	0.376	0.165	0.092	0.822	0.662	0.258
0.285	0.393	0.005	0.000	0.000	0.676	0.916	0.004	0.000	0.010	0.066	0.461	0.804	0.241	0.600	0.816	0.549	0.330	0.020	0.683
0.978	0.189	0.217	0.106	0.003	0.310	0.397	0.789	0.187	0.017	0.098	0.521	0.907	0.471	0.618	0.908	0.323	0.811	0.169	0.568
0.016	0.061	0.327	0.004	0.038	0.805	0.029	0.583	0.536	0.883	0.328	0.000	0.323	0.018	0.790	0.966	0.418	0.856	0.155	0.636
0.594	0.312	0.770	0.358	0.054	0.451	0.236	0.032	0.242	0.210	0.174	0.942	0.628	0.100	0.800	0.882	0.447	0.988	0.001	0.272
0.582	0.796	0.042	0.000	0.014	0.274	0.381	0.001	ND	ND	ND	0.143	0.269	0.936	0.138	0.714	0.400	0.061	0.060	0.015
0.296	0.320	0.002	0.000	0.000	0.675	0.377	0.276	0.433	0.622	0.587	0.627	0.086	0.425	0.452	0.634	0.286	0.010	0.000	0.457

PHA-665752	PHA-665752	PHA-665752	AZD6244	AZD6244	AZD6244	PLX4720	PLX4720	PLX4720	Bortezomib	Bortezomib	Bortezomib	Lapatinib	Lapatinib	Lapatinib	Vandetanib	Vandetanib	Vandetanib	Trastuzumab	Trastuzumab
1	**2**	**3**	**1**	**2**	**3**	**1**	**2**	**3**	**1**	**2**	**3**	**1**	**2**	**3**	**1**	**2**	**3**	**1**	**2**
0.361	0.872	0.093	0.724	0.812	0.191	0.459	0.774	0.966	0.920	0.566	0.234	0.441	0.651	0.663	0.577	0.433	0.371	0.572	0.396
0.576	0.506	0.529	0.003	0.044	0.018	0.413	0.980	0.834	0.977	0.805	0.859	0.441	0.936	0.724	0.538	0.338	0.383	0.460	0.371
0.252	0.374	0.054	0.536	0.165	0.628	0.611	0.853	0.686	0.908	0.009	0.783	0.547	0.564	0.265	0.273	0.085	0.541	0.752	0.586
0.284	0.310	0.022	0.707	0.001	0.002	0.033	0.007	0.514	0.057	0.002	0.000	0.700	0.046	0.716	0.255	0.011	0.012	0.927	0.672
0.524	0.110	0.000	0.408	0.113	0.815	0.014	0.183	0.352	0.236	0.379	0.555	0.306	0.061	0.096	0.765	0.461	0.295	0.315	0.033
0.711	0.442	0.002	0.476	0.164	0.724	0.384	0.939	0.542	0.514	0.065	0.920	0.433	0.573	0.332	0.177	0.022	0.553	0.502	0.866
0.608	0.316	0.105	0.002	0.000	0.002	0.112	0.011	0.603	0.208	0.036	0.000	0.289	0.017	0.244	0.163	0.002	0.002	0.619	0.890
0.782	0.115	0.005	0.095	0.013	0.378	0.771	0.361	0.469	0.390	0.683	0.534	0.030	0.128	0.113	0.688	0.010	0.115	0.056	0.019
0.817	0.520	0.238	0.527	0.040	0.546	0.553	0.931	0.826	0.388	0.205	0.848	0.972	0.538	0.418	0.727	0.128	0.438	0.732	1.000
0.549	0.550	0.327	0.005	0.755	0.430	0.167	0.084	0.256	0.238	0.031	0.745	0.870	0.736	0.631	0.315	0.018	0.400	0.453	0.487
0.292	0.126	0.000	0.207	0.013	0.153	ND	ND	ND	0.358	0.015	0.161	0.863	0.300	0.094	0.819	0.096	0.422	0.601	0.676
0.083	0.907	0.248	0.056	0.086	0.594	0.081	0.609	0.123	0.820	0.014	0.074	0.633	0.154	0.101	0.079	0.040	0.014	0.009	0.254
0.192	0.638	0.001	0.000	0.002	0.086	0.000	0.065	0.353	0.733	0.989	0.670	0.971	0.017	0.219	0.000	0.001	0.002	0.502	0.386
0.494	0.337	0.085	0.133	0.181	0.300	0.307	0.707	0.090	0.959	0.015	0.007	0.527	0.030	0.096	0.203	0.022	0.022	0.541	0.935
0.719	0.275	0.000	0.002	0.033	0.058	0.096	0.989	0.881	0.397	0.778	0.585	0.997	0.060	0.411	0.012	0.000	0.006	0.191	0.467
0.144	0.966	0.001	0.098	0.255	0.477	0.108	0.162	0.066	0.162	0.262	0.129	0.201	0.721	0.092	0.255	0.120	0.084	0.148	0.661
0.621	0.637	0.493	0.073	0.004	0.041	0.185	0.467	0.744	0.193	0.107	0.842	0.561	0.096	0.133	0.005	0.000	0.015	0.484	0.732
0.068	0.000	ND	0.122	0.056	0.081	0.719	0.610	0.776	0.306	ND	0.770	0.801	0.447	0.900	0.823	ND	0.002	0.196	ND
0.317	0.524	0.342	0.038	0.008	0.220	0.616	0.023	0.023	0.542	0.474	0.389	0.082	0.019	0.091	0.023	0.000	0.001	0.481	0.406
0.000	0.000	ND	0.208	0.019	0.123	0.559	0.514	0.575	0.217	ND	0.774	0.206	0.472	0.716	0.704	ND	0.674	0.000	ND
0.402	0.555	0.083	0.051	0.006	0.795	0.328	0.000	0.016	0.509	0.386	0.046	0.312	0.001	0.108	0.233	0.009	0.002	0.822	0.443
0.000	0.000	ND	0.106	0.110	0.097	0.630	0.273	0.962	0.099	ND	0.848	0.159	0.343	0.768	0.448	ND	0.072	0.009	ND
0.382	0.423	0.008	0.358	0.218	0.008	ND	ND	ND	ND	ND	ND	ND	ND	ND	0.853	0.102	0.048	ND	ND
0.228	0.408	0.000	0.825	0.217	0.157	0.567	0.933	0.698	0.048	0.000	0.000	0.365	0.014	0.971	0.232	0.000	0.000	0.163	0.258
0.870	0.045	0.005	0.239	0.043	0.040	0.719	0.193	0.433	0.329	0.008	0.002	0.472	0.724	0.291	0.463	0.365	0.000	0.342	0.255
0.736	0.573	0.458	0.626	0.709	0.001	0.611	0.578	0.060	0.003	0.000	0.000	0.024	0.603	0.264	0.066	0.000	0.000	0.007	0.000
0.000	0.138	0.493	0.228	0.027	0.000	0.397	0.211	0.240	0.401	0.008	0.000	0.381	0.650	0.621	0.535	0.617	0.007	ND	ND
0.385	0.491	0.001	0.560	0.002	0.001	0.933	0.986	0.679	0.284	0.000	0.000	0.431	0.033	0.094	0.013	0.000	0.000	0.000	0.004
0.258	0.381	0.394	0.259	0.004	0.000	0.266	0.369	0.223	0.306	0.001	0.000	0.443	0.719	0.750	0.535	0.727	0.000	0.295	0.787

Trastuzumab	17-AAG	17-AAG	17-AAG	Everolimus	Everolimus	Everolimus	Rosuvastatin-Ca	Rosuvastatin-Ca	Rosuvastatin-Ca	Thalidomide	Thalidomide	Thalidomide	Atorvastatin-Ca	Atorvastatin-Ca	Atorvastatin-Ca	Indometacin	Indometacin	Indometacin	Cetuximab
3	**1**	**2**	**3**	**1**	**2**	**3**	**1**	**2**	**3**	**1**	**2**	**3**	**1**	**2**	**3**	**1**	**2**	**3**	**1**
0.645	0.717	0.921	0.490	0.520	0.534	0.751	0.279	0.140	0.249	0.942	0.972	0.867	0.246	0.081	0.201	0.101	0.452	0.489	0.988
0.694	0.405	0.174	0.865	0.766	0.770	0.903	0.372	0.205	0.990	0.278	0.424	0.334	0.183	0.572	0.655	0.698	0.371	0.090	0.013
0.658	0.814	0.688	0.148	0.093	0.461	0.088	0.297	0.474	0.006	0.301	0.241	0.391	0.412	0.788	0.200	0.327	0.831	0.604	0.310
0.803	0.487	0.279	0.003	0.323	0.273	0.260	0.590	0.388	0.951	0.136	0.226	0.342	0.327	0.402	0.614	0.899	0.002	0.007	0.086
0.209	0.697	0.001	0.000	0.078	0.647	0.646	0.752	0.001	0.002	0.785	0.758	0.325	0.066	0.000	0.004	0.288	0.306	0.273	0.080
0.397	0.333	0.493	0.618	0.172	0.893	0.285	0.537	0.593	0.072	0.175	0.232	0.363	0.372	0.719	0.144	0.465	0.389	0.247	0.152
0.505	0.395	0.460	0.000	0.394	0.398	0.407	0.540	0.434	0.651	0.139	0.211	0.338	0.363	0.406	0.535	0.768	0.016	0.326	0.037
0.170	0.436	0.004	0.000	0.026	0.290	0.580	0.783	0.131	0.037	0.942	0.917	0.326	0.191	0.011	0.008	0.053	0.010	0.867	0.024
0.084	0.558	0.478	0.140	0.199	0.600	0.212	0.185	0.275	0.003	0.177	0.225	0.350	0.279	0.825	0.155	0.314	0.782	0.745	0.934
0.180	0.167	0.430	0.407	0.177	0.330	0.143	0.426	0.257	0.366	0.141	0.212	0.351	0.384	0.382	0.265	0.512	0.231	0.001	0.004
0.530	0.018	0.313	0.029	ND	ND	ND	0.573	0.409	0.001	0.897	0.769	0.317	0.368	0.038	0.001	0.841	0.036	0.558	0.000
0.001	0.417	0.409	0.172	0.958	0.371	0.014	0.899	0.635	0.081	0.289	0.224	0.328	0.764	0.853	0.454	0.392	0.664	0.575	0.015
0.005	0.370	0.002	0.001	0.913	0.256	0.113	0.086	0.064	0.020	0.328	0.272	0.341	0.315	0.002	0.007	0.493	0.005	0.005	0.000
0.005	0.960	0.690	0.374	0.601	0.987	0.883	0.830	0.928	0.185	0.306	0.208	0.336	0.458	0.683	0.534	0.724	0.496	0.820	0.185
0.010	0.672	0.000	0.003	0.091	0.734	0.170	0.723	0.090	0.047	0.227	0.256	0.334	0.295	0.071	0.008	0.771	0.214	0.362	0.003
0.001	0.539	0.888	0.763	0.621	0.273	0.067	0.769	0.114	0.037	0.257	0.197	0.333	0.659	0.042	0.342	0.892	0.623	0.002	0.020
0.008	0.403	0.032	0.020	0.590	0.999	0.068	0.026	0.007	0.078	0.302	0.269	0.336	0.079	0.000	0.037	0.704	0.322	0.000	0.001
0.486	0.479	0.188	0.430	0.928	0.458	0.324	0.766	0.513	0.070	ND	ND	ND	0.188	0.754	0.349	0.193	0.259	0.060	0.893
0.940	0.749	0.255	0.033	0.500	0.004	0.000	0.172	0.073	0.001	ND	ND	ND	0.168	0.353	0.005	0.000	0.002	0.000	0.356
0.052	0.006	0.019	0.255	0.399	0.584	0.390	0.903	0.323	0.001	ND	ND	ND	0.945	0.630	0.019	0.244	0.588	0.001	0.319
0.820	0.180	0.513	0.122	0.273	0.012	0.001	0.032	0.000	0.000	ND	ND	ND	0.273	0.098	0.003	0.711	0.757	0.000	0.109
0.000	0.076	0.229	0.368	0.630	0.217	0.037	0.064	0.612	0.060	ND	ND	ND	0.001	0.036	0.178	0.625	0.921	0.063	0.675
#DIV/0!	0.130	0.002	0.617	0.188	0.759	0.155	0.094	0.001	0.002	ND	ND	ND	ND	ND	ND	ND	ND	ND	0.118
0.007	0.030	0.000	0.000	0.404	0.060	0.005	0.185	0.067	0.000	0.362	0.417	0.632	0.891	0.397	0.064	0.373	0.029	0.001	0.034
0.002	0.126	0.026	0.245	0.604	0.129	0.064	0.374	0.501	0.051	0.488	0.664	0.631	0.418	0.636	0.101	0.609	0.004	0.496	0.000
0.001	0.510	0.165	0.004	0.257	0.002	0.001	0.214	0.018	0.000	0.567	0.610	0.563	0.225	0.727	0.155	0.513	0.205	0.042	0.219
ND	0.248	0.000	0.104	0.578	0.139	0.276	0.602	0.559	0.107	0.536	0.568	0.557	0.440	0.361	0.510	0.681	0.165	0.022	0.227
0.001	0.279	0.030	0.006	0.065	0.563	0.154	0.327	0.027	0.009	0.729	0.751	0.342	0.012	0.875	0.014	0.530	0.018	0.009	0.358
0.048	0.487	0.591	0.088	0.601	0.446	0.950	0.689	0.817	0.048	0.300	0.191	0.333	0.430	0.710	0.039	0.385	0.297	0.001	0.006

Cetuximab 2	Cetuximab 3	Sorafenib 1	Sorafenib 2	Sorafenib 3	Sunitinib 1	Sunitinib 2	Sunitinib 3	Erlotinib 1	Erlotinib 2	Erlotinib 3
0.619	0.942	0.417	0.342	0.439	0.305	0.934	0.706	0.371	0.340	0.735
0.021	0.855	0.265	0.257	0.612	0.659	0.106	0.025	0.393	0.727	0.189
0.660	0.293	0.136	0.206	0.721	0.678	0.753	0.612	0.370	0.979	0.440
0.032	0.905	0.207	0.299	0.011	0.399	0.007	0.273	0.730	0.184	0.003
0.084	0.025	0.184	0.832	0.531	0.390	0.002	0.136	0.156	0.002	0.001
0.557	0.242	0.174	0.224	0.735	0.906	0.882	0.549	0.193	0.881	0.846
0.004	0.608	0.174	0.230	0.011	0.280	0.003	0.429	0.607	0.000	0.000
0.005	0.003	0.064	0.091	0.029	0.173	0.012	0.110	0.132	0.000	0.004
0.423	0.144	0.081	0.201	0.843	0.372	0.815	0.720	0.689	0.117	0.796
0.928	0.726	0.232	0.610	0.821	0.434	0.718	0.417	0.734	0.012	0.447
0.017	0.002	ND	ND	ND	0.822	0.029	0.003	0.012	0.000	0.019
0.010	0.612	0.197	0.000	0.054	0.551	0.125	0.015	0.795	0.001	0.049
0.000	0.000	0.000	0.149	0.014	0.017	0.077	0.024	0.356	0.000	0.003
0.003	0.081	0.007	0.000	0.025	0.620	0.037	0.044	0.020	0.001	0.037
0.000	0.001	0.083	0.007	0.011	0.613	0.448	0.008	0.167	0.000	0.000
0.687	0.401	0.047	0.000	0.019	0.956	0.408	0.276	0.778	0.000	0.000
0.000	0.009	0.063	0.070	0.012	0.101	0.361	0.936	0.564	0.004	0.013
0.053	0.000	0.358	ND	0.624	0.956	0.522	0.021	0.712	0.064	0.039
0.018	0.000	0.424	0.158	0.043	0.624	0.798	0.966	0.010	0.000	0.032
0.615	0.633	0.699	ND	0.222	0.126	0.525	0.111	0.969	0.162	0.095
0.024	0.000	0.000	0.000	0.012	0.129	0.576	0.758	0.084	0.001	0.012
0.591	0.021	0.342	ND	0.625	0.536	0.171	0.002	0.375	0.236	0.061
0.395	0.167	ND	ND	ND	0.722	0.242	0.345	0.621	0.005	0.916
0.021	0.373	0.203	0.007	0.014	0.399	0.558	0.649	0.601	0.001	0.023
0.000	0.161	0.113	0.026	0.015	0.075	0.272	0.708	0.003	0.000	0.120
0.907	ND	0.000	0.054	0.008	0.093	0.016	0.003	0.259	0.884	0.533
0.748	0.184	0.302	0.000	0.008	0.295	0.141	0.664	0.424	0.000	0.182
0.052	0.008	0.073	0.027	0.020	0.002	0.012	0.000	0.029	0.023	0.000
0.944	0.889	0.135	0.003	0.008	0.982	0.120	0.010	0.252	0.013	0.038

Supplementary Table S3.
List of the drugs included in the library and tested on HME-1 cell lines. The table also includes the target on which compounds are known to act.

Drug	Target(s)
Erlotinib	EGFR
Cetuximab	EGFR
Trastuzumab	HER2
Canertinib (CI-1033)	HER1, HER2 and HER4
Lapatinib (GW572016)	EGFR, HER2
Vandetanib (ZD6474)	EGFR + VEGFR
Sunitinib	VEGFR-1,2, PDGFR, c-kit , Flt3
Sorafenib	VEGFR-1,2,3 PDGFR,RAF, c-kit
Vatalanib	VEGFR-1,2, PDGFR, c-kit , c-Fms
Cediranib (AZD-2171)	VEGFR-1,2,3
NVP-AEW541	IGF-1R
BMS-536924	IGF1R&FAK
PHA-665752	MET
L744832	FTS
PLX4720	BRAF
AZD6244 (ARRY-142886)	MEK
Bosutinib	ABL, SRC
Saracatinib	ABL, SRC
NVP-BEZ235	PI3K
GDC-0941	PI3K
XL-765	PI3K
Perifosine	AKT
MK-2206	AKT
Everolimus	mTOR
17-AAG	HSP-90
Bortezomib	Proteasome
NVP TAE 684	ALK
Valproic Acid	Histone deacetylase
Vorinostat (SAHA)	Histone deacetylase
Decitabine	DNA methyltransferase
BI-2536	Polo-like kinase
GW 843682X	Polo-like kinases-1&3
STF-62247	VHL
Obatoclax	Bcl2 Antagonist
Elesclomol	Apoptosis
Olaparib AZD2281	PARP
Thalidomide	TNF-α; IL-6
Lenalidomide	TNF-α; IL-6
Indomethacin	COX
OSU-03012	PDK-1
Atorvastatin	HMG-COA reductase
Rosuvastatin	HMG-COA reductase
Metformin	AMPK